Title
MODELING GEOTHERMAL SYSTEMS

Authors
Witherspoon, P.A.
Neuman, S.P.
Sorey, M.L.
et al.

Publication Date
1975-05-01

Presented at the International Meeting on
Geothermal Phenomena and Its Applications,
Accademia Nazionale dei Lincei, Rome, Italy,
March 3 - 5, 1975

MODELING GEOTHERMAL SYSTEMS

P. A. Witherspoon, S. P. Neuman, M. L. Sorey, and
M. J. Lippmann

May 1975

Prepared for the U. S. Energy Research and
Development Administration under Contract W-7405-ENG-48

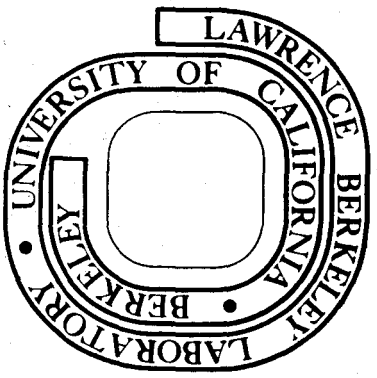

DISCLAIMER

MODELING GEOTHERMAL SYSTEMS

by

P. A. Witherspoon,[1] S. P. Neuman,[1] M. L. Sorey[2]
and M. J. Lippmann[3]

ABSTRACT

Geothermal systems are receiving more and more attention as an alternative source of energy and, consequently, there is growing interest in attempting to understand their nature and behavior. One approach to this problem is to attempt to deduce the physical behavior of such systems using a mathematical model. This paper presents the governing equations for energy and mass transfer in porous media that must be solved in using such models. Fundamental concepts that have been developed for factors that affect the development of free and forced convection in geothermal systems under natural conditions are reviewed. The results of modeling geothermal systems during exploitation using lumped-parameter and distributed-parameter models are also presented.

---

[1] Lawrence Berkeley Laboratory and Department of Civil Engineering, University of California, Berkeley.

[2] U. S. Geological Survey, Menlo Park, California.

[3] Department of Civil Engineering, University of California, Berkeley.

INTRODUCTION

Geothermal systems are receiving more and more attention as an alternative source of energy and, consequently, there is growing interest in attempting to understand their nature and behavior. One approach to this problem is to attempt to deduce the physical behavior of such systems using a mathematical model. Such a model consists of a set of equations that describe the processes occurring within the system and the solution to these equations subject to conditions that prevail at a particular site.

The model approach has two important applications: (1) the geothermal system under natural conditions before being disturbed by man, and (2) the geothermal system during exploitation. Natural geothermal systems have been investigated by a great many workers. The main thrust of such studies has been to understand how geothermal systems can form and persist within the earth's crust.

The mathematical model can also be applied to the problem of evaluating the behavior of a geothermal system during exploitation. One of the most critical problems in developing such systems as a viable source of energy is that of determining that a particular reservoir once discovered is capable of producing significant quantities of energy over meaningful periods of time. The model is one of several tools that can be used to analyze this problem. During the early stages, the model may be crude, but its application in parametric analysis of the field data can provide valuable limits as to what can be expected. As more data become available, the model can be refined and such engineering questions as well spacing, optimum rates of fluid withdrawal and effects of reinjection can be studied.

In this review, we shall restrict our attention to hydrothermal systems, i.e., to geothermal systems involving water. We shall pay particular attention

to hydrothermal-convection systems, in which most of the heat is transferred in circulating fluids rather than by heat conduction. Two broad types of hydrothermal systems are recognized: (1) hot-water, and (2) vapor-dominated (White 1973).

In the hot-water type, water is the continuous phase throughout the system and thus provides the pressure control. Continuity of the liquid phase is evident from reservoir pressures that are near hydrostatic and the presence of soluble salts that are not found to any significant degree in low-pressure steam. In the vapor-dominated type, steam is the continuous, pressure-controlling phase, although there is general agreement that liquid water must also be present (Facca and Tonani, 1964, Elder, 1965; Craig, 1966; James, 1968; Marinelli, 1969; Sestini, 1970; White et al., 1971).

An intriguing question arises concerning the initial conditions of vapor-dominated systems. At depths below 350 m, they all tend to have temperatures near 240°C and pressures near 35 kg/cm^2, which usually means well below hydrostatic (White, 1973). This uniformity in the initial conditions is believed to be strongly influenced by the maximum enthalpy of saturated steam (James, 1968; Sestini, 1970; White at al., 1971).

The material and thermodynamic properties of the different components of geothermal systems are an important consideration in any attempt to develop realistic models of such systems. Fig. 1 presents a pressure-enthalpy diagram for pure water at pressures up to 700 kg/cm^2 and temperatures up to 500°C. Dissolved salts are, of course, common in geothermal waters and studies on the effect of salinity on heat capacity (Nevens and Pool, 1964; Likke and Bromley, 1973), density (Haas, 1970), viscosity (Matthews and Russell, 1967, Fig. G4), and maximum thermal gradient (Haas, 1971) of brines are available. Helgeson (1968) has investigated the thermodynamic characteristics of the Salton Sea geothermal system where the highest concentrations, approaching 300,000 ppm, have been found.

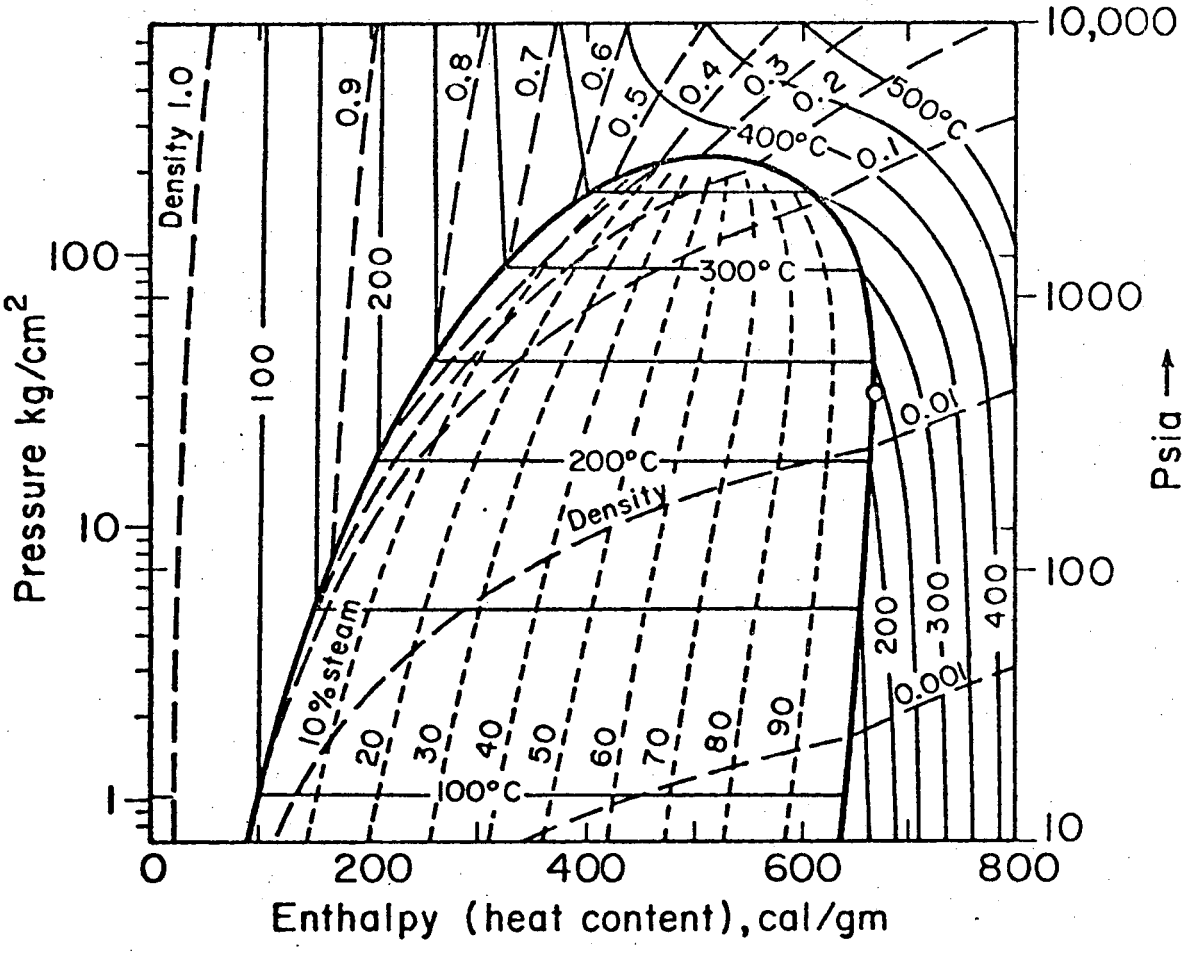

Fig. 1. Pressure-enthalpy diagram for pure water and vapor, showing contours of equal temperature, density and mass proportions of steam to water. Open circle indicates maximum enthalpy of saturated steam, 670 cal/gm at 236°C and 31.8 kg/cm^2 (after White et al., 1971).

The thermal properties of rocks are very important since the dominant fraction of the total energy in a geothermal system is in the solid matrix. Comprehensive tables of these properties for dry rocks have recently been compiled by Kappelmeyer and Haenel (1974). Thermal conductivities for most dry rocks range from 4 to 10 mcal/cm sec ^{o}C; specific heats are approximately 0.2 cal/g ^{o}C; and thermal diffusivities range from 5 to 15 cm^2/sec. Kappelmeyer and Haenel also include the effects on these thermal properties of temperature and pressure.

The thermal conductivity of fluid-saturated rocks is dependent on the conductivities of the dry rock and the saturating fluid as well as the physical properties of the rock. Anand et al. (1973) and Somerton et al. (1974) have shown how thermal conductivities increase with brine saturation and become more sensitive to temperature change. They discuss correlations for predicting thermal conductivity from other rock properties.

The hydraulic properties of the rocks are also important since they control the fluid movement. The absolute values of permeability and porosity for rocks vary considerably and must be measured or estimated for any given system. A few workers have studied the thermal effects and report that the absolute permeability tends to decrease, sometimes significantly, with increasing temperature (Greenberg et al., 1968; Sanyal et al., 1972; Casse, 1974). There are also important effects of temperature on relative permeability (Edmonson, 1965; Davidson, 1969; Poston et al., 1970; Weinbrandt et al., 1972; Lo and Mungan, 1973; Ramey et al., 1974). In studying the effects of pressure, a number of workers (Knutson and Bohor, 1963; Brace et al., 1968; Vairogs et al., 1971) have suggested that permeability depends only on effective stress; that is, permeability is dependent only on the difference between hydrostatic confining pressure and internal pore pressure. However, Zoback and Byerlee (1975), have recently shown that pore pressure has a significantly larger effect on permeability under isothermal conditions than does confining pressure.

In this review of the problems involved in modeling geothermal reservoirs, we shall first present the governing equations for energy and mass transfer in porous media. Then we shall consider some of the fundamental concepts that have been developed for factors that affect the development of free and forced convection in geothermal systems under natural conditions. Lastly, we shall review the results of several efforts that have been made to model geothermal systems during exploitation.

GOVERNING EQUATIONS

Let us consider a porous medium completely saturated with a single-component homogeneous fluid which can be either in a liquid or gaseous state. The liquid and gas phases are assumed to be separated locally by a distinct interface due to capillarity. Since mass may be transferred from one phase to another across the interface by vaporization or condensation, it is convenient to write a single mass balance equation for both phases

$$\frac{\partial}{\partial t}\left(\phi\, S^L \rho^L + \phi\, S^G \rho^G\right) = -\frac{\partial}{\partial x_i}\left(\rho^L v_i^L + \rho^G v_i^G\right) \tag{1}$$

Rate of mass accumulation — Convective mass flux

All mathematical symbols appearing in the text are macroscopic quantities defined over a representative elementary volume of the porous medium. For a definition of these symbols the reader is referred to the Nomenclature.

It is generally believed that capillary pressure between the phases is small relative to absolute pressure, and as each phase may flow independently, we shall assume Darcy's law in the form

$$v_i^L = -\frac{k_{ij}\, k_r^L}{\mu^L}\left(\frac{\partial p}{\partial x_j} - \rho^L g_j\right) \tag{2}$$

$$v_i^G = -\frac{k_{ij}\, k_r^G}{\mu^G}\left(\frac{\partial p}{\partial x_j} - \rho^G g_j\right) \tag{3}$$

The relative permeabilities k_r^L and k_r^G are functions of fluid saturation and, as mentioned earlier, they may also be functions of temperature. Recent studies (Coats et al., 1974) indicate the latter effect is important and should be taken into account.

An energy balance equation must also be considered, and one way to derive such an equation in terms of macroscopic quantities is to follow an averaging procedure (see Appendix). Equation A21 is a general form of the macroscopic energy balance for the case where irreversible viscous dissipation of mechanical energy and transfer of kinetic energy between fluid and rock are neglected. An attempt to derive a set of more general equations considering mechanical interaction between rock and fluid has been reported recently by Brownell et al. (1975). It is customary to assume that not only is the capillary pressure zero, but also that the solid, liquid, and gas are locally in thermal equilibrium. In this case (A21) reduces to (A22) which can be written more conveniently without the angular brackets as

$$\frac{\partial}{\partial t}\left[\phi\, S^L \rho^L e^L + \phi\, S^G \rho^G e^G + (1-\phi)\, \rho^S e^S\right] = \frac{\partial}{\partial x_i}\left(\kappa_{ij}^{eff} \frac{\partial T}{\partial x_j}\right)$$

Rate of internal energy accumulation — Conductive and dispersive internal energy flux

$$- \frac{\partial}{\partial x_i}\left(\rho^L e^L v_i^L + \rho^G e^G v_i^G\right) - p \frac{\partial}{\partial x_i}\left(v_i^L + v_i^G\right) \qquad (4)$$

Convective internal energy flux — Rate of reversible mechanical energy (work) conversion to internal energy

Our mathematical analysis indicates that

$$\kappa_{ij}^{eff} = \phi\, S^L \kappa_{ij}^L + \phi\, S^G \kappa_{ij}^G + (1-\phi)\, \kappa^S \delta_{ij} \qquad (5)$$

Laboratory experiments show that κ_{ij}^{eff} is not always given by (5) (Combarnous and Bories, 1973, Fig. 6), thus implying that the assumption of local thermal equilibrium may not always hold. Moreover, as mentioned earlier, thermal conductivity may also be a function of temperature.

Equation 4 can be reformulated in terms of enthalpy by writing $h - p/\rho$

instead of e and, as shown in (A25), one then has

$$\frac{\partial}{\partial t}\left[\phi\, S^L \rho^L h^L + \phi\, S^G \rho^G h^G + (1-\phi)\, \rho^S h^S\right] = \frac{\partial}{\partial x_i}\left(\kappa_{ij}^{eff} \frac{\partial T}{\partial x_j}\right)$$
$$- \frac{\partial}{\partial x_i}\left(\rho^L h^L v_i^L + \rho^G h^G v_i^G\right) + \frac{\partial(\phi p)}{\partial t} + \left(v_i^L + v_i^G\right)\frac{\partial p}{\partial x_i} \qquad (6)$$

This is identical with an expression reported earlier by Mercer et al. (1974) except that we have omitted source terms.

In the particular case where only one fluid phase is present, the energy equation can be conveniently expressed in terms of temperature and, as shown in (A31), one obtains for a liquid saturated medium

$$\left[\phi\, \rho^L c_v^L + (1-\phi)\, \rho^S c_v^S\right]\frac{\partial T}{\partial t} = \frac{\partial}{\partial x_i}\left(\kappa_{ij}^{eff} \frac{\partial T}{\partial x_j}\right)$$
$$- \rho^L v_i^L c_v^L \frac{\partial T}{\partial x_i} - T\left(\frac{\partial p}{\partial T}\right)_v \frac{\partial v_i^L}{\partial x_i} \qquad (7)$$

A similar expression holds for a medium saturated with gas.

The above equations must be supplemented by equations of state relating the thermodynamic variables e, h, ρ, μ, S, p, T. Here it is customary to assume that all phases are in equilibrium and that thermodynamic relationships between macroscopic quantities remain the same as those between the equivalent point quantities. In particular, the macroscopic saturations S^L and S^G are assumed to be uniquely determined by the pressure and total energy or enthalpy of the fluid (both phases combined). In other words, whenever two phases occur simultaneously at a point in the system, their p-T relationship is uniquely determined by conditions at the vapor pressure.

Although capillary pressure is neglected in the governing equations, it may still have an important effect on thermodynamic properties. Ramey et al. (1973) explain that the vapor-pressure curve in the presence of uneven capillary surfaces may be lower than that quoted in steam tables. Calhoun et al. (1949) showed that in consolidated sandstones the vapor-pressure curve at 36°C is significantly

affected by a decreasing liquid saturation. However, Cady (1969) and Bilhartz (1971) were unable to confirm this effect on unconsolidated sands with temperatures between 121°C and 240°C. The effect of capillary pressure therefore remains unclear.

Some geothermal systems such as those in Imperial Valley (California) involve waters of high salinity which cannot be treated as a homogeneous fluid because salt concentrations are not uniform. In this case the mass as well as energy balance equations (see Appendix) may have to be modified to include a term for dispersive mass flux and an additional equation for mass balance of the solute. Another complication may arise due to coupling between thermal and chemical gradients which modifies the form of Fourier's law of heat conduction (Dufour effect) and Fick's first law of diffusion (Soret effect). The presence of salts may also cause a slight lowering of the vapor-pressure curve (Haas, 1971; Ramey et al., 1973), and this effect becomes progressively more important as boiling proceeds, due to the increasing salt concentration (White, 1973). Very little is known about the behavior of these so-called thermohaline systems, but a few theoretical analyses have appeared (Nield, 1968, 1974; Rubin, 1973, 1975 a,b,c). The discussion that follows will be concerned solely with homogeneous fluids.

GEOTHERMAL SYSTEMS UNDER NATURAL CONDITIONS

Fundamental Characteristics of Free Convection

Mathematical modeling related to geothermal systems has long centered on problems of convective heat transfer in a homogeneous porous layer heated from below. Pioneering work on this subject has been performed independently by Horton and Rogers (1945), Lapwood (1948), and Goguel (1953). Their efforts were directed primarily toward developing criteria for the onset of convection currents in a horizontal and laterally infinite layer. These analyses followed the pattern of earlier work by Rayleigh (1916), Jeffreys (1930), and others who showed that in a static layer of viscous fluid the critical temperature gradient (i.e., the

gradient at which cellular or Bénard convection is formed) depends on thermal conductivity, thermal coefficient of expansion, kinematic viscosity, thickness of the layer, and the boundary conditions. When fluid cannot enter or leave the system, the resulting flow pattern is referred to as "natural" or "free" convection. When fluid flow is entirely due to hydraulic forces acting at the boundaries, the result is known as "forced" convection, whereas "mixed" convection includes a combination of both phenomena. Early work on the subject was restricted to free convection.

In reviewing the mathematical approach to free convection in porous media, we find it instructive to follow a recent development by Beck (1972). Consider a rectangular box of porous material resting on a horizontal surface and saturated by a homogeneous liquid (see Fig. 2). The vertical sides are thermally insulated (i.e., adiabatic), and the lower ($z = 0$) and upper ($z = D$) surfaces are isothermal. Temperature T_1 at the bottom is greater than T_o at the top, and all boundaries are impermeable to fluid.

In most analytical studies of thermal convection, it is customary to invoke the Boussinesq approximation that spatial as well as temporal variations in fluid density can be neglected except for buoyancy effects (i.e., everywhere except in the gravity term in the equation of motion). In addition, all coefficients in the governing equations are assumed to be constant scalars. Under these conditions the mass balance equation 1 reduces to

$$\frac{\partial v_i}{\partial x_i} = 0 \tag{8}$$

In writing Darcy's law, it is customary to replace ρ by $\rho_o [1 - \beta(T - T_o)]$ in the gravity term and add a term including the time derivative of velocity (compare with Eq. 2),

$$\frac{1}{\phi}\frac{\partial v_i}{\partial t} + \frac{\mu}{k\rho_o} v_i = [1 - \beta (T - T_o)] g_i - \frac{1}{\rho_o}\frac{\partial p}{\partial x_i} \tag{9}$$

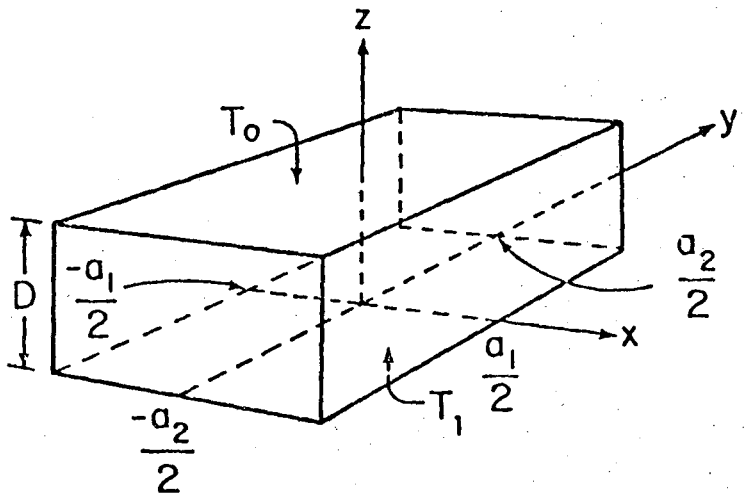

Fig. 2. Rectangular box of porous media saturated with a homogeneous liquid.

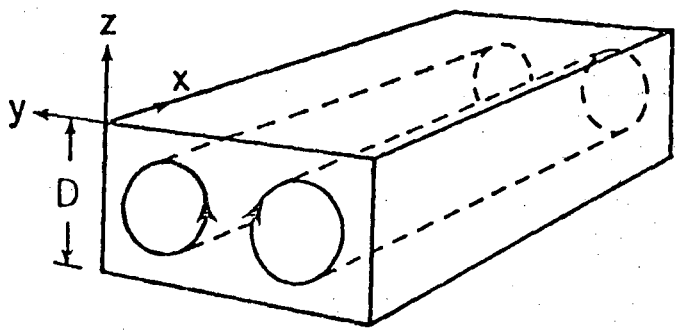

Fig. 3. Two convective rolls in rectangular box heated from below.

Energy balance is usually expressed by a simplified version of equation 7, and Beck writes, using our notation

$$(\rho c_v)^{eff} \frac{\partial T}{\partial t} = - \rho_o c_v v_i \frac{\partial T}{\partial x_i} + \kappa^{eff} \frac{\partial^2 T}{\partial x_i^2} \tag{10}$$

where $(\rho c_v)^{eff} = \phi \rho_o c_v + (1-\phi) \rho^S c_v^S$.

Initially, the system is assumed to be in static equilibrium so that the pressure is hydrostatic. Thus,

$$v_i^o = (0, 0, 0) \text{ and } T^o = T_1 + (T_o - T_1) \frac{z}{D} \tag{11}$$

Under these conditions, there are no convective currents and the system is said to be "statically stable." Let a small volume of fluid suddenly be brought from elevation $z = 0$ to a higher elevation $z > 0$, thus superimposing a disturbance (v_i', T', p') upon the "basic state" (v_i^o, T^o, p^o). We now want to determine whether or not the system is "dynamically stable," i.e., whether this disturbance will die out or build up to the level of a discernible convective current. Equations 8 - 11 as well as the boundary conditions must be satisfied by the disturbed state as well as by the basic state. Thus, by writing these equations first in terms of ($v_i^o + v_i'$, $T^o + T'$, $p^o + p'$) and then in terms of (v_i^o, T^o, p^o), we can subtract the second set from the first to obtain

$$\frac{\partial v_i'}{\partial x_i} = 0 \tag{12}$$

$$\frac{1}{\phi} \frac{\partial v_i'}{\partial t} + \frac{\mu}{k\rho_o} v_i' = - \beta T' g_i - \frac{1}{\rho_o} \frac{\partial p'}{\partial x_i} \tag{13}$$

$$(\rho c_v)^{eff} \frac{\partial T'}{\partial t} = - \rho_o c_v v_i' \frac{\partial (T^o+T')}{\partial x_i} + \kappa^{eff} \frac{\partial^2 T'}{\partial x_i^2} \tag{14}$$

subject to the boundary conditions

$$v_i' n_i = 0 \quad \text{at} \quad x = \pm \tfrac{1}{2} a_1; \; y = \pm \tfrac{1}{2} a_2; \; z = 0, D \tag{15}$$

$$T' = 0 \quad \text{at} \quad z = 0, D \tag{16}$$

$$\frac{\partial T'}{\partial x_i} n_i = 0 \quad \text{at} \quad x = \pm \tfrac{1}{2} a_1; \quad y = \pm \tfrac{1}{2} a_2 \tag{17}$$

where n_i is the unit outward normal to the boundaries of the box.

To reduce these equations to a dimensionless form it is helpful to use the following dimensionless groups:

$$\text{Thermal diffusivity:} \quad \alpha = \kappa^{eff}/(\rho_o c_v) \tag{18}$$

$$\text{Rayleigh number:} \quad Ra = k \rho_o g \beta (T_1 - T_o) D/(\mu\alpha) \tag{19}$$

$$\text{Prandtl number:} \quad Pr = k \alpha \rho_o/(\mu D^2 \phi) \tag{20}$$

$$\text{Heat capacity ratio:} \quad H = (\rho c_v)^{eff}/(\rho_o c_v) \tag{21}$$

$$\text{Aspect ratios:} \quad D_1 = a_1/D; \quad D_2 = a_2/D \ . \tag{22}$$

The Rayleigh number relates buoyancy to viscous retardation, whereas the Prandtl number relates thermal diffusivity to viscous retardation. If we also define a set of dimensionless variables

$$\left.\begin{array}{llll} \nu_i = D v_i'/(\alpha Ra^{\frac{1}{2}}) & \theta = T'/(T_1 - T_o) & p_D = k p'/(\mu \alpha Ra^{\frac{1}{2}}) & \\ \tau = t\alpha/D^2 & X = x/D & Y = y/D & Z = z/D \end{array}\right\} \tag{23}$$

we can rewrite (12) - (17) as

$$\frac{\partial \nu_i}{\partial X_i} = 0 \tag{24}$$

$$Pr \frac{\partial \nu_i}{\partial \tau} + \nu_i = \underbrace{Ra^{\frac{1}{2}} \theta \delta_{i3}}_{\substack{\text{zero for} \\ i = 1,2}} - \frac{\partial p_D}{\partial X_i} \ . \tag{25}$$

$$H \frac{\partial \theta}{\partial \tau} = - Ra^{\frac{1}{2}} \nu_i \frac{\partial \theta}{\partial X_i} + \underbrace{Ra^{\frac{1}{2}} \nu_i \delta_{i3}}_{\substack{\text{zero for} \\ i = 1,2}} + \frac{\partial^2 \theta}{\partial X_i^2} \tag{26}$$

$$\nu_i n_i = 0 \quad \text{at} \quad X = \pm \tfrac{1}{2} D_1; \quad Y = \pm \tfrac{1}{2} D_2; \quad Z = 0, 1 \tag{27}$$

$$\theta = 0 \qquad \text{at} \quad Z = 0,\ 1 \tag{28}$$

$$\frac{\partial \theta}{\partial X_i} n_i = 0 \quad \text{at} \quad X = \pm \tfrac{1}{2} D_1;\ \ Y = \pm \tfrac{1}{2} D_2 \tag{29}$$

The dynamic stability of this system can be investigated by a linear method or by an energy approach. In the linear approach the disturbances are assumed to be small enough for second-order terms to be neglected. The conditions for marginal stability (i.e., stability just at the onset of convection) can thus be determined from the above equations after reducing (25) and (26) to

$$- Ra^{\frac{1}{2}} \theta \, \delta_{i3} + \nu_i = - \frac{\partial p_D}{\partial X_i} \tag{30}$$

$$Ra^{\frac{1}{2}} \nu_i \, \delta_{i3} = - \frac{\partial^2 \theta}{\partial X_i^{\,2}} \tag{31}$$

According to the linear theory, the critical Rayleigh number, $Ra_c^{\,linear}$, is the smallest eigenvalue of the resulting problem. However, this theory indicates only a necessary condition for stability, and the true critical Rayleigh number may therefore be smaller, $Ra_c^{\,true} \leq Ra_c^{\,linear}$.

The energy method was first applied to porous media by Westbrook (1969) and was later extended by Wankat and Schowalter (1970) and Beck (1972). Stability is established relative to arbitrary disturbances subject only to the equation of continuity and corresponding boundary conditions. Since stability actually depends on a more restricted class of disturbances satisfying (24) - (29), the critical Rayleigh number obtained may be too conservative and we therefore have $Ra_c^{\,energy} \leq Ra_c^{\,true}$. However, in the particular case considered here, both methods lead to the same eigenvalue problem and therefore $Ra_c^{\,linear} = Ra_c^{\,energy}$.

Beck showed that the eigenvalue problem has separable eigenfunctions, the velocity components of which are

$$\nu_1 = \sin\left[(\tfrac{1}{2}\, m\pi)(1 + 2X/D_1)\right] \cos\left[(\tfrac{1}{2}\, n\pi)(1 + 2Y/D_2)\right] U(Z)$$

$$\nu_2 = \cos\left[(\tfrac{1}{2}\, m\pi)(1 + 2X/D_1)\right] \sin\left[(\tfrac{1}{2}\, n\pi)(1 + 2Y/D_2)\right] V(Z) \qquad (32)$$

$$\nu_3 = \cos\left[(\tfrac{1}{2}\, m\pi)(1 + 2X/D_1)\right] \cos\left[(\tfrac{1}{2}\, n\pi)(1 + 2Y/D_2)\right] \sin(\ell\pi Z)$$

$$m,n = 0, 1, 2, \ldots; \quad \ell = 1, 2, \ldots .$$

where U(Z) and V(Z) are functions of Z only. The corresponding critical Rayleigh numbers are

$$Ra_c = \pi^2 \min_{\ell,m,n} (b + \ell^2/b)^2 = \pi^2 \min_{m,n} (b + b^{-1})^2 \qquad (33)$$

where $b = \left[(m^2/D_1^{\,2}) + (n^2/D_2^{\,2})\right]^{\frac{1}{2}}$ and $\ell = 1$.

Equation 33 shows that the critical Rayleigh number depends entirely on aspect ratios D_1 and D_2. The minimum possible value of Ra_c is $4\pi^2$ corresponding to $b = 1$. Lapwood (1948) obtained $Ra_c = 4\pi^2$ for the case of a laterally infinite layer, thus indicating that vertical walls tend to stabilize the system. However, Ra_c remains nearly equal to $4\pi^2$ unless D_1 or D_2 are less than about 0.8, as may happen in a narrow and tall box.

Geometry becomes more important when one considers the mode of convection. It is evident from (32) that when $m = 0$, the horizontal velocity ν_1 vanishes, which gives rise to n convective cells known as "rolls" (see Fig. 3). Since Ra_c corresponds to $\ell = 1$, ν_3 in (32) is identically zero only at $Z = 0$ and $Z = 1$, and thus the vertical extent of each roll is equal to the height of the box. A typical temperature profile in a plane perpendicular to the axis of such a roll is shown in Fig. 4. Rolls are invariably preferred over three-dimensional cells whenever the height D is not the smallest dimension. When rolls do form, they are usually parallel to the shorter side, although the overriding rule is for the number of rolls and the direction of their axes to be such that each roll has the closest approximation to a square cross-section as possible. Three-dimensional cells are preferred when a_1, a_2, and D are nearly the same size (i.e., a cube)

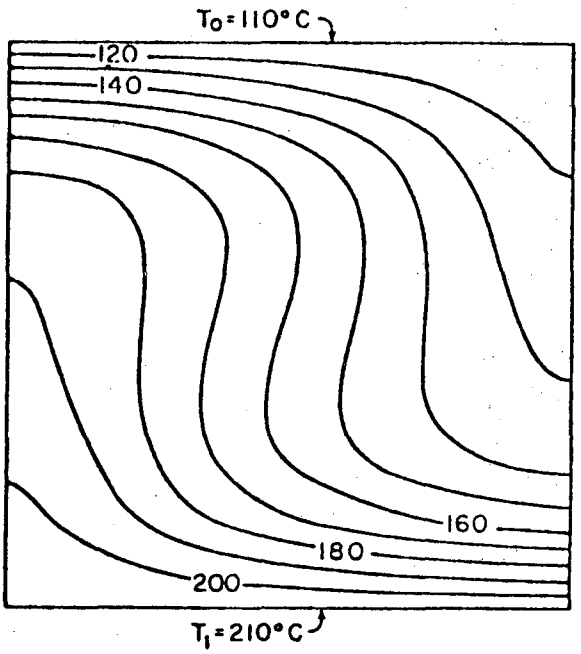

Fig. 4. Typical temperature distribution in plane perpendicular to axis of single convective roll with Ra = 100 (after Sorey, 1975).

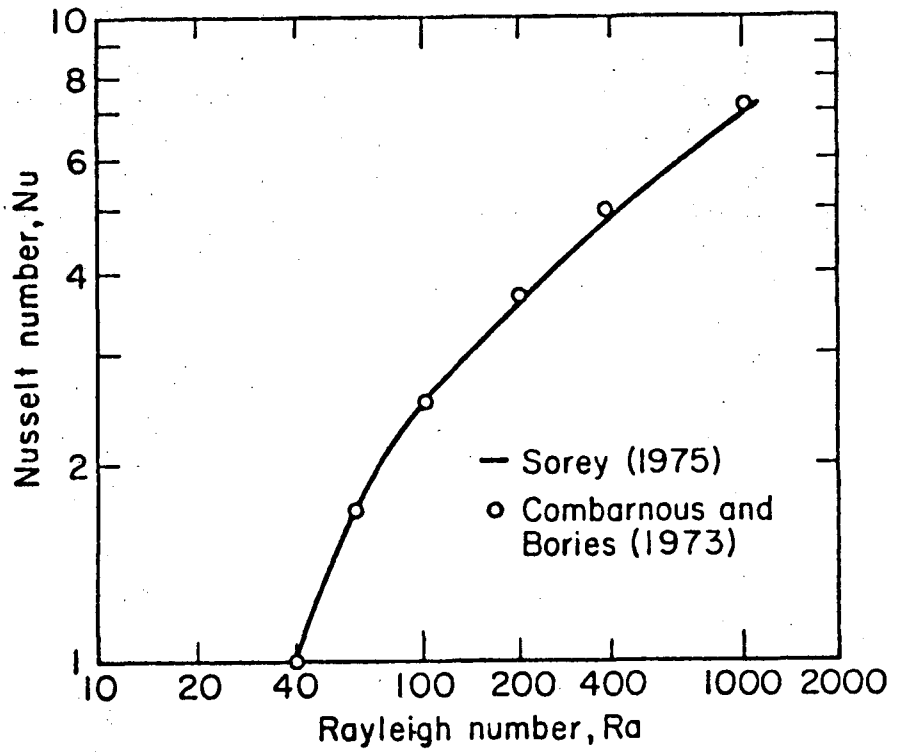

Fig. 5. Maximum Nusselt number versus Rayleigh number for cellular convection in a laterally infinite layer (after Sorey, 1975).

or when the height is less than both lateral dimensions. For a cube, the motion resembles a toroid with vertical axis through the center of the box. For further details regarding these conclusions, the reader is referred to Beck (1972).

It is important to recognize that all of these results have been obtained from an analysis of marginal stability and are therefore limited to Rayleigh numbers in the immediate neighborhood of Ra_c. In order to obtain results for higher Rayleigh numbers one must either perform experiments or solve the governing equations by an appropriate analytical or numerical technique. A large number of such studies concerned with both steady and nonsteady state situations have been reported in the literature and we shall try to summarize briefly some of the most important aspects of this work.

One effect of convective motion is to increase the rate of vertical heat transfer through the system. This is measured by the Nusselt number, Nu, which is defined as the ratio of total heat flow in the presence of convection to that by conduction only. For Rayleigh numbers less than the critical value, Nu = 1; otherwise $Nu \geq 1$. Fig. 4 shows the steady state temperature distribution corresponding to a roll at Ra = 100 for which Nu = 2.6.

According to the criterion of Platzman (1965), a system will tend to establish a mode of convection which maximizes the rate of heat transfer. At Rayleigh numbers near Ra_c, this means that cells with nearly square cross sections are preferred. However, at large Rayleigh numbers, Combarnous and Bories (1973) and Horne and O'Sullivan (1974) show that the preferred cell width depends on Ra, with aspect ratios of 0.5, .33, and .25 corresponding to Rayleigh numbers of 280, 400 and 700, for layers with no restraining side walls. Similar effects of reduced cell width with increased Ra are observed for box models with restraining side walls. Combarnous and Bories (1973), Holst and Aziz (1972b), and Sorey (1975) found that Nusselt numbers are nearly the same for two- and three-dimensional motions in stable

convection states. The relationship between Ra and the maximum Nusselt number for a laterally infinite layer is plotted in Fig. 5.

Sorey (1975) further indicates that the cellular pattern and Nusselt number at steady state may depend on the initial conditions in the box. Using uniform initial temperature and pressure distributions in a square (two-dimensional problem) with Ra = 100 led to development of two cells with Nu = 2.2. With a non-uniform temperature distribution, the result was a single cell with Nu = 2.6. Horne and O'Sullivan (1974) report from numerical as well as laboratory experiments that for a uniform initial temperature distribution, heating the lower boundary slowly insteady of instantaneously results in unicellular rather than multicellular motion. In other words, the mode of convection is not necessarily unique but may depend on the past history of the system. A hysteresis effect has also been noted by Elder (1967) and Karra (1968).

As Ra increases to 280, the system tends to develop a more favorable mode of convection and, as a result, the fluid may start fluctuating. These fluctuations will be irregular when the boundary conditions are uniform, but may develop into stable oscillations when the boundaries are heated in a nonuniform fashion. Horne and O'Sullivan (1974) report isotherms during a single oscillation when half of the bottom boundary has an elevated uniform temperature as shown in Fig. 6. A rough calculation for the Wairakei geothermal region indicates that, if the depth is 5 km, the oscillations would have a time constant on the order of 1000 years, and it would therefore be practically impossible to detect them.

Free Convection Models

Numerous authors have attempted to extend the analysis of free convection to more realistic systems. There are, however, several complicating factors. The concept of a critical Rayleigh number may not apply in geothermal reservoirs where horizontal temperature variations undoubtedly exist along bounding surfaces. Free convection is then set up for any value of Ra > 0, although its effect on the

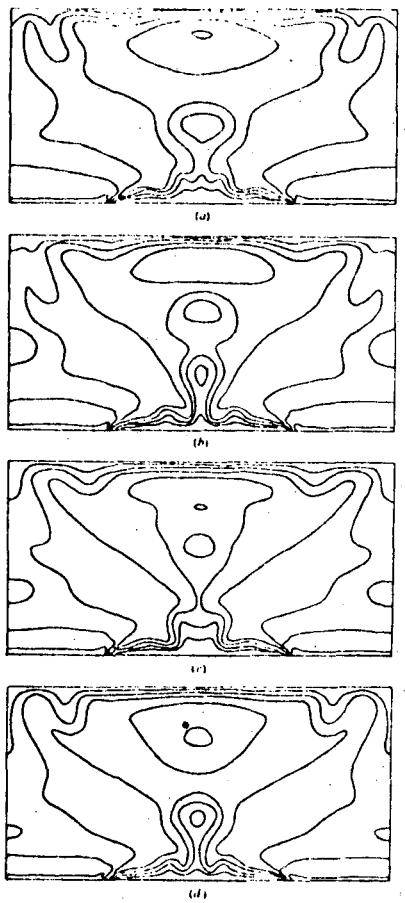

Fig. 6. Isotherm plots at equal intervals of time during a single stable oscillation with Ra = 750 (after Horne and O'Sullivan, 1974).

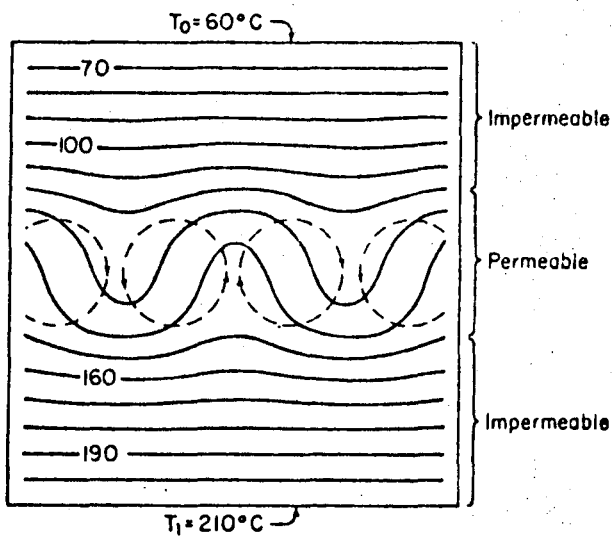

Fig. 7. Distortion of isotherms due to convection in central permeable layer (after Sorey, 1975).

thermal and hydrologic regimes should be negligible unless Ra is large. Donaldson (1968b) estimates that in geothermal areas Ra is in the range of 500-5000. Caltagirone et al. (1971) suggest the concept of a local Rayleigh number which varies spatially within the reservoir to account for the fluctuating convective motions observed.

Combarnous and Bories (1973) evaluated the effects of assuming thermal equilibrium between solid and fluid phases (Eqs. 4-7) for systems with Rayleigh numbers well above theoretical critical values. Comparisons of experimental and numerical results for the relationship between Ra and Nu numbers using various combinations of porous media and fluid types indicate that the assumption of thermal equilibrium between solid and fluid phases is adequate for Ra at least as high as 2000.

Holst and Aziz (1972a) and Sorey (1975) investigated effects of temperature and pressure-dependent parameters on heat transfer in convecting systems. For water, the dominant influence is the viscosity variation such that as the temperature difference across the permeable layer T_1-T_o increases, the effective Rayleigh number increases over the value calculated from equation 19 using parameters computed at $T = T_o$. The Nusselt number would be correspondingly greater and the critical Rayleigh number, lower than for the constant parameter case. Alternatively, if parameters are evaluated at $T = (T_1 + T_o)/2$, values of Ra_c and the Ra versus Nu relationship still vary with $T_1 - T_o$ due to the nonlinearity in the temperature dependence of c_v, ρ, and μ (Sorey, 1975). In contrast, realistic variations in fluid density with pressure were found to have negligible effects on the cellular convection problem.

Studies have also been made on the effect of various uniform boundary conditions at the surfaces of the homogeneous region on Ra_c. Lapwood (1948) investigated a laterally infinite layer in which the lower boundary is impermeable and the upper boundary is maintained at constant pressure and found that $Ra_c = 27.1$. Lapwood also found that when the upper boundary is a perfectly conducting free

surface, then $Ra_c = 4\pi^2$; but when it becomes an imperfect conductor, then $27.1 \leq Ra_c \leq 4\pi^2$. A table of Ra_c values for a variety of uniform boundary conditions is given by Nield (1968) and in all cases, $Ra_c \leq 4\pi^2$.

Donaldson (1962) analyzed free convection in a two-layer system in which a permeable layer was underlain by an impermeable but thermally conductive layer of equal thickness. This removes the assumption of an isothermal surface at the bottom of the convecting layer. Sorey (1975) extended the analysis to a three-layer system with impermeable zones above and below the reservoir and found, in agreement with Donaldson's results, that vertical heat transfer rates in the multilayer systems were significantly less than in the single-layer system for the same values of Ra. The critical Rayleigh number was also less for the multilayer systems. Fig. 7 shows how temperatures within the impermeable layers are distorted by convection in the central layer.

Some work has also been done on the problem of an inclined system bounded by isothermal surfaces (Combarnous and Bories, 1973; Kaneko et al., 1974). Combarnous and Bories show that, since the temperature gradient and gravity are no longer colinear, the fluid is constantly moving regardless of the Rayleigh number. In a layer of infinite lateral extent, the tendency at low Rayleigh numbers is to develop unicellular convection parallel to the slope. If this is considered the stable state, instabilities develop at critical Rayleigh numbers which depend on the angle of inclination. When this angle is less than 15°, $Ra_c \approx 40$ and the mode of convection is similar to that observed in a horizontal layer. Above this lower limit, Ra_c increases rapidly with the angle of inclination and convective movements take the form of adjacent coils climbing upslope. Fluctuating conditions develop at higher and higher Rayleigh numbers ($Ra \geq 240 - 280$ for horizontal layer) as the angle of inclination increases. The case of the inclined box is more complex (Holst and Aziz, 1972a; Kaneko et al., 1974).

Wooding (1963) and McNabb(1965) have studied the effect of localized heat sources on the formation of vertical jet flows. McNabb developed a boundary layer theory for convective flow over a finite circular "hot plate" at the bottom of a semi-infinite porous medium. He estimated the amount of heat convected from the hot plate as a function of its temperature and suggested that a similar approach could be used to evaluate the rate of cooling of a magma chamber beneath a water saturated porous formation.

Cheng and Lau (1974) have investigated steady state free convection in a vertical cross section of an unconfined aquifer in which the position of the water table is not known a priori. The aquifer is assumed to rest on an impermeable horizontal heat source of variable temperature and is bounded on its sides by vertical isothermal surfaces of constant hydraulic head, representing contact with the ocean on a volcanic island. Dispersion and gravity effects due to variations in salt content between fresh water and sea water (mixing occurs by virtue of the vertical boundary conditions) are implicitly neglected. By solving a linearized version of the governing equations, the authors show that pressure in the aquifer remains nearly hydrostatic. Temperature is greatly affected by the size of the heat source but its location is less important. There is a noticeable upwelling of the water table directly above the heat source, which depends primarily on vertical temperature gradients and nature of the heat source.

Much additional literature on various theoretical and experimental aspects of free convection in homogeneous media is available. Holst (1970) has published an extensive review of the literature and the state of the art has been summarized more recently by Combarnous and Bories (1973). For subsequent developments, the reader should consult the works of Fernandez (1972), Holst and Aziz (1972 a,b), Masuoka (1972), Palm et al. (1972), Sun et al. (1972), Gupta and Joseph (1973), Cheng and Lau (1974), Combarnous and Bories (1974), Horne and O'Sullivan (1974), Kaneko et al. (1974), Straus (1974), Yen (1974), Weber (1975 a,b), and Sorey (1975).

Pipe Models

An alternative concept for convection in geothermal areas is the pipe system in which the fluid no longer flows through a homogeneous layer but is channeled through zones of relatively high permeability. Such zones may be caused by fissures or fractures which are known to control local phenomena such as springs, fumaroles, and geysers. As discussed by Einarsson (1942), Bodvarsson (1961), and Donaldson (1970), the occurrence and distribution of thermal areas in Iceland and New Zealand could be controlled by variations in permeability as well as by spatial distribution of the heat source.

Einarsson (1942) and Bodvarsson (1961) discuss the thermal areas of Iceland in terms of pipe systems involving deep circulation of water (2 to 3 km) and discharge in hot springs. Elder (1966) analyzed hydrothermal systems in Iceland and New Zealand using lumped parameter and multi-dimensional models to quantify the general features of heat and mass transfer. White (1957, 1961) used pipe systems to explain the chemical composition of waters associated with volcanic and hydrothermal systems.

Donaldson (1968b, 1970) suggests the model in Fig. 8 for a hot-water geothermal system. The model consists of cold reservoirs recharged from the surface, a vertical column through which hot water flows, and a permeable horizontal channel connecting the two. The surrounding medium is assumed impermeable, and heat supplied at the lower boundary maintains the density imbalance and resulting convective motion. Though the model is oversimplified, Donaldson's analysis allows for throughflow from recharge to discharge areas and secondary (circulatory) convection in the upflow column. Gross characteristics of hydrothermal systems are simulated by adjusting temperatures at the base of the model, dimensions and permeability of the vertical column, and resistance to flow in the remainder of the pipe system.

Mathematical description of the model involves the single phase, steady state equivalents of (1) and (7) which are solved by numerical relaxation for the boundary conditions shown in Fig. 8. Uniform thermal properties are assumed throughout

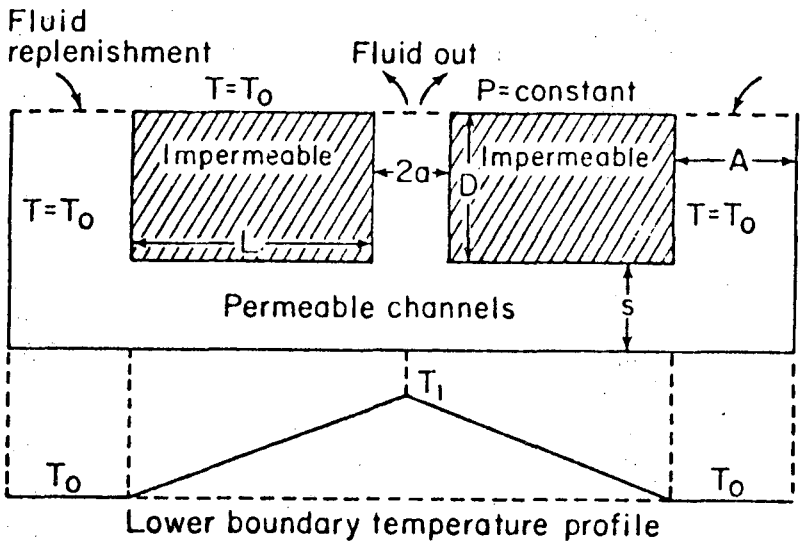

Fig. 8. Pipe model for hot-water geothermal system (after Donaldson, 1968b).

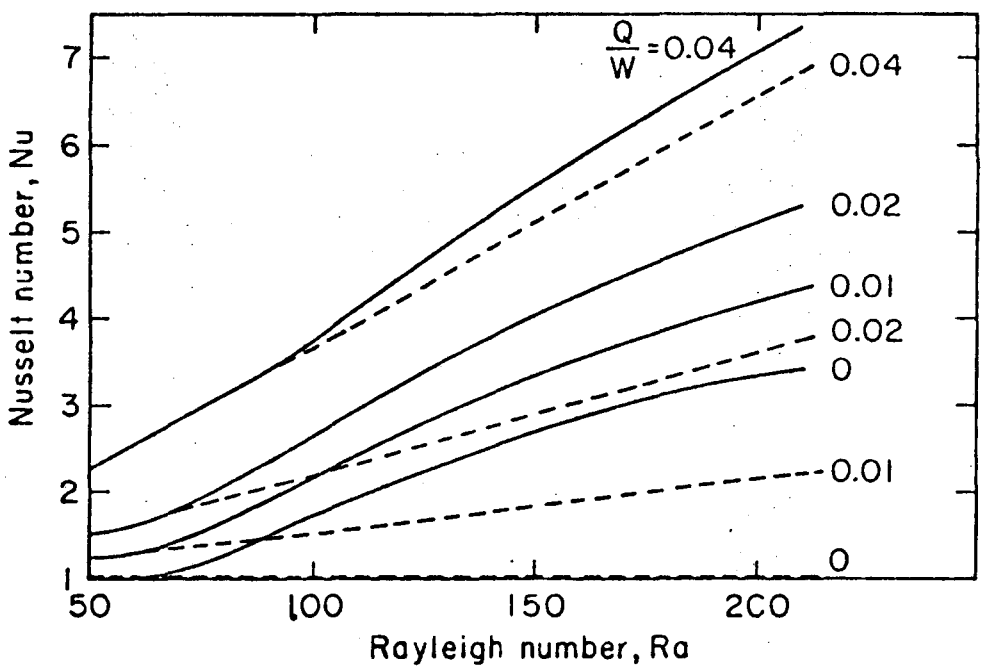

Fig. 9. Nusselt number versus Rayleigh number for combined through and circulatory flows in vertical column with 2a/D = 0.5. Solid lines show combined effect, dashed lines show throughflow effect only (after Donaldson, 1970).

and constant values for k and μ are used in each of the permeable channels. In the absence of secondary convection in the upflow column, the mean mass flow rate is given by

$$Q = \frac{\rho_o \, k \, \beta \, g \, (T_m - T_o)}{(\mu/\rho) \, b} \tag{34}$$

where T_m = mean temperature in the column and $b = 1 + aL/sD + A/D$. It is not clear from Donaldson's analysis whether μ/ρ is determined at T_o or T_m. Fig. 9 illustrates the relationship between Ra and Nu with throughflow and secondary convection for a column aspect ratio $2a/D = 0.5$. Here $W = \rho_o \, k \, \beta \, g \, (T_1 - T_o)/(\mu/\rho)$ is a measure of the maximum possible throughflow from buoyancy unbalance alone. Hence, $Q/W = [(T_m - T_o)/(T_1 - T_o)] \, (1/b)$. It is seen from Fig. 9 that the heat transferred by circulatory flow decreases markedly as the throughflow increases. Fig. 10 illustrates how throughflow in a column with $2a/D = 0.2$ and $Q/W = 0.05$ tends to sweep the circulatory motion up the channel.

Sorey (1975) modeled heat and liquid mass transfer in hot spring systems using the two-dimensional models shown in Fig. 11. Transient and steady state conditions were simulated numerically to determine conductive heat losses from the vertical conduit and its effect on temperature T_{sp} of water discharging at the spring. The lower boundary was formed by the top of a reservoir with water at temperature T_b, and the upper boundary was the land surface at temperature T_s. The relationships between dimensionless temperature drop, $1 - \theta_{sp}$, and the dimensionless mass flow rates for the circular conduit, m_c, and the fault plane conduit, m_p, are plotted in Fig. 12.

Expressions for the total conductive heat loss are $[2\pi \, \kappa^{eff} \, D \, (T_b - T_s) \, m_c \, (1 - \theta_{sp})]$ for the cylinder and $[2 \, \kappa^{eff} \, D \, (T_b - T_s) \, m_p \, (1 - \theta_{sp}) \, L/a]$ for the plane. The plane model applies where fluid rises in a fault zone whose lateral extent is considerably greater than the discharge area of the hot springs. Comparing the two models for the same total mass flow, the fault plane model has greater

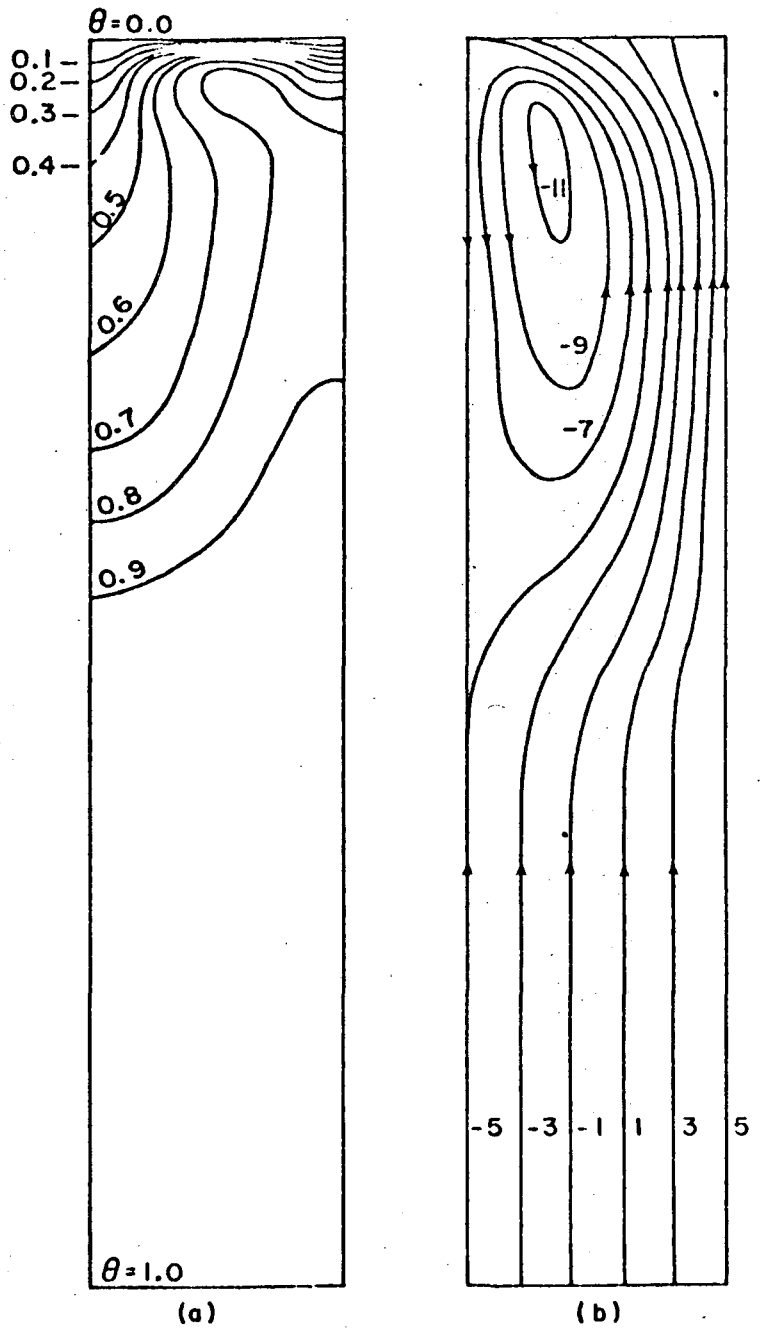

Fig. 10. Effect of throughflow on circulatory convection with Ra = 420, 2a/D = 0.2, Q/W = 0.05; (a) isotherms normalized such that $0 \leq \theta \leq 1.0$, (b) streamlines in arbitrary units (after Donaldson, 1970).

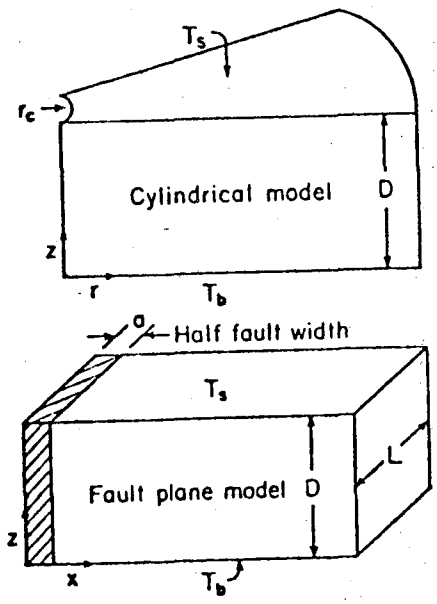

Fig. 11. Two-dimensional models for hot spring systems (after Sorey, 1975).

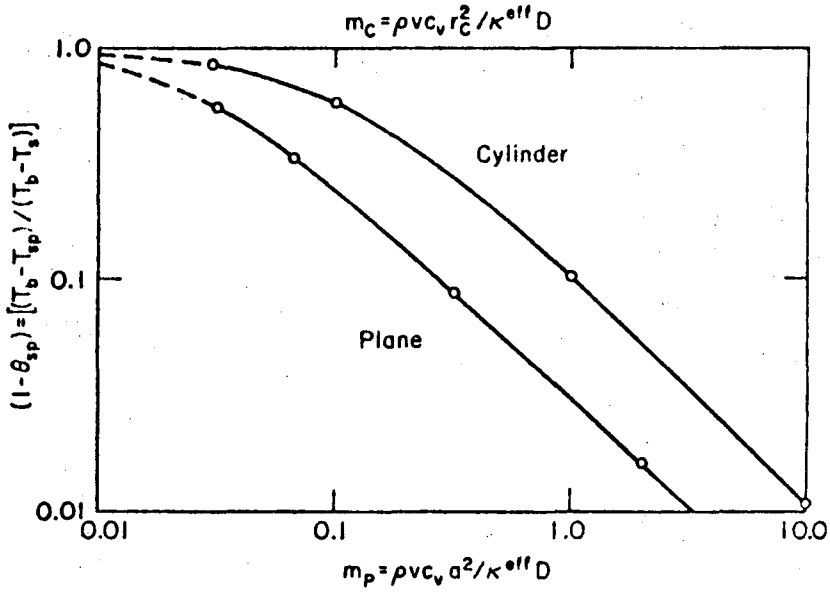

Fig. 12. Dimensionless temperature drop, $1-\theta_{sp}$, versus dimensionless mass flow rates for circular conduit, m_c, and fault plane conduit, m_p, in hot spring systems (after Sorey, 1975).

heat loss and more temperature drop than the cylindrical conduit model.

The steady-state temperature distribution in a fault plane model with a spring discharge of 100 lpm is shown in Fig. 13. Distortion of the temperatures due to convective motion in the conduit is confined to a zone of about 1 km on either side of the fault. At the land surface, the conductive heat flux near the spring is approximately 50 heat flow units (50 μcal/sec cm^2) and decreases to about 3.4 heat flow units as distance exceeds 1 km. These results were obtained using κ^{eff} = 2×10^{-3} cal/cm sec ^{o}C and c_v = 1 cal/gm ^{o}C.

Analysis of the transient behavior of these systems (Sorey, 1975) shows that periods of 30,000 years or more are required for the conductive thermal regime to reach equilibrium following the geologic development of the spring system. Somewhat shorter time periods are required if convective motions in the rock surrounding the spring conduit are considered. Simulations under these conditions are described by Sorey (1975).

Analysis of pipe models has been extended by Elder (1966) and Donaldson (1968a, 1970) to include boiling in the upflow channel. Elder has developed relationships between mass flow rate, fluid enthalpy, resistance to flow, and the energy supplied by a heat source for channeled circulation caused by buoyancy differences between recharge and discharge areas. He concludes that for systems with large energy input or large resistance, the discharge (mass flow) is not sufficient to transport the energy unless the fluid moves in the form of steam. With low energy inputs or small resistance, the circulating fluid should remain a liquid except for a shallow zone which may contain steam. This approach has been applied to the Tuscany thermal areas near Lardarello, Italy, and the Taupo systems in New Zealand.

Donaldson's (1968a) work involves steady flow of a boiling liquid in a vertical channel. The remainder of the circulation system including the heat source is considered only as controlling temperature, pressure, and mass flux at the bottom of the discharge channel. Lateral heat conduction is neglected so that the

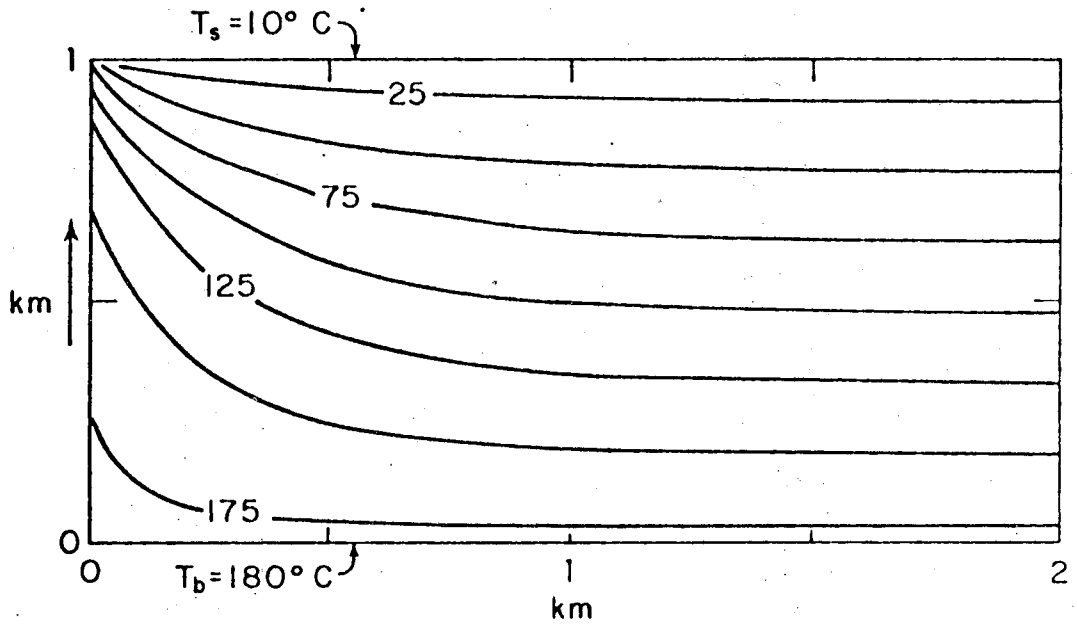

Fig. 13. Distortion of steady-state isotherms in vertical fault plane model with discharge = 100 lpm, a = 10 m, L = 1 km, and Ra = 0 (after Sorey, 1975).

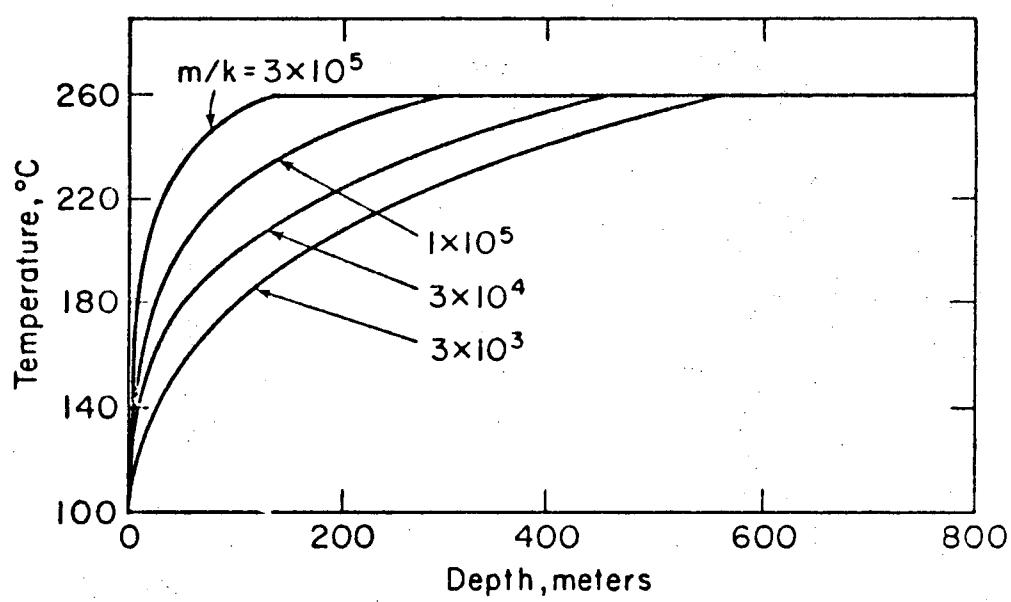

Fig. 14. Temperature versus depth in a boiling system as a function of m/k (after Donaldson, 1968a).

equations are one-dimensional. For the case of uniform permeability and small mass flow rate, only liquid flow is considered. Comparison of the resultant pressure-depth relations with saturation pressure curves indicates that boiling will not occur for systems with $c_v\ m/\kappa^{eff} \leq 7 \times 10^{-5}\ cm^{-1}$, where m is mass flux per unit area. When this critical value is exceeded, boiling must occur in the upper section of the channel.

Two-phase flow in this upper region is described by the one-dimensional, steady state forms of equations 1 - 3 and 6 without the pressure terms. At the interface between the two-phase and liquid-saturated regions, the boundary conditions are constant mass flux and constant temperature equal to that at the channel base. Thus, the lower region is treated as isothermal, and in the upper region, temperature and pressure are related by the vapor pressure curve for water. The equations are solved analytically to yield temperature and pressure, water fraction, and water and steam flow rates as functions of depth. The controlling parameter in these relationships is m/k as seen in Fig. 14. Thus, the onset of boiling is indicated by the value of $c_v\ m/\kappa^{eff}$, whereas when two-phase conditions exist, the controlling parameter is m/k. Effects of vertical heat conduction are significant only if κ^{eff}/k is greater than 3×10^8 cal/cm^3 sec ^oC. Donaldson concludes that once boiling commences, it must extend some 200 - 500 meters downward and hence this two-phase region must be considered in studying geothermal systems. Two-phase conditions in columns with variations in vertical permeability have also been discussed by Donaldson (1968a, 1970).

GEOTHERMAL SYSTEMS DURING EXPLOITATION

Lumped-Parameter Models

The concept of a lumped-parameter model provides one of the simplest means for describing behavior of a geothermal system during exploitation. The basic idea is to view the entire system as a perfect mixing cell for both mass and energy so that spatial variations in concentration can be neglected. Instead of

considering the internal distribution of mass and energy, attention is restricted to the total amounts generated within the system as well as that crossing the boundaries. Since time is the only independent variable, the system can be characterized mathematically by a set of ordinary differential equations or an equivalent set of algebraic expressions representing total mass and energy balance.

The first and best known lumped-parameter model of a producing geothermal reservoir was developed by Whiting and Ramey (1969). Their system has a bulk volume V and contains vapor, water, and rock. Figure 15 is a schematic diagram of the system from which a simple mass balance yields

$$M_c - M_o = M_e - M_p - M_\ell \tag{35}$$

where M_c = current mass of water (vapor + liquid) in place, M_o = initial mass of water in place, M_e = influx of liquid (no vapor is assumed to enter the system), M_p = mass of water (vapor + liquid) produced, and M_ℓ = mass of water (vapor + liquid) lost by leakage. Water may flow in from an adjacent aquifer or leak out of the system via steam vents, springs, wild wells, etc. The water influx, M_e, is represented by a linear combination of terms each of which is the product of a theoretical time-dependent response function characterizing a certain aquifer flow geometry (hemispherical, linear, or radial) and pressure. These calculations further assume that the liquid inflow is isothermal with constant enthalpy, h_e.

In the energy balance calculation the system is assumed to be in complete thermodynamic equilibrium. According to the first law of thermodynamics one then has

$$\underbrace{M_c\, e_c - M_o\, e_o}_{\text{Internal energy change in fluid}} + \underbrace{V\,(1-\phi)(\rho c_v)^{eff}\,(T_c - T_o)}_{\text{Internal energy change in solid rock}} = \underbrace{-Q}_{\text{Net conductive heat influx}} + \underbrace{M_e\, h_e - M_p\, h_p - M_\ell h_\ell}_{\text{Net convective enthalpy influx}} \tag{36}$$

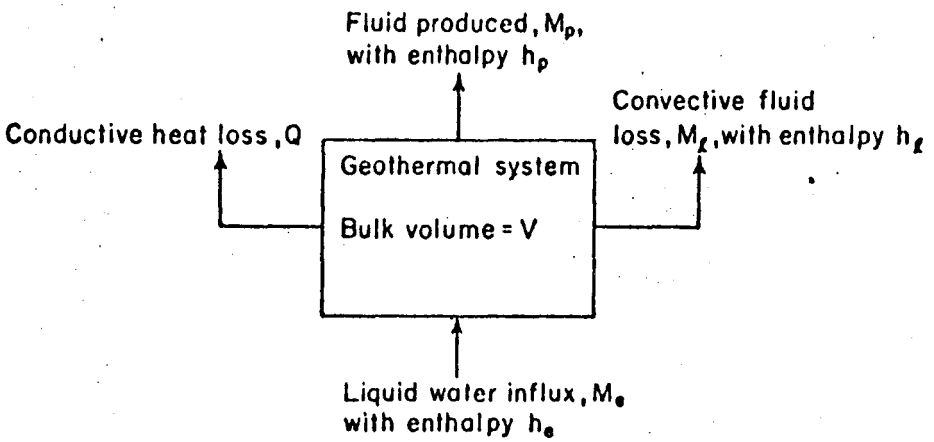

Fig. 15. Schematic diagram of lumped-parameter model for geothermal systems (after Whiting and Ramey, 1969).

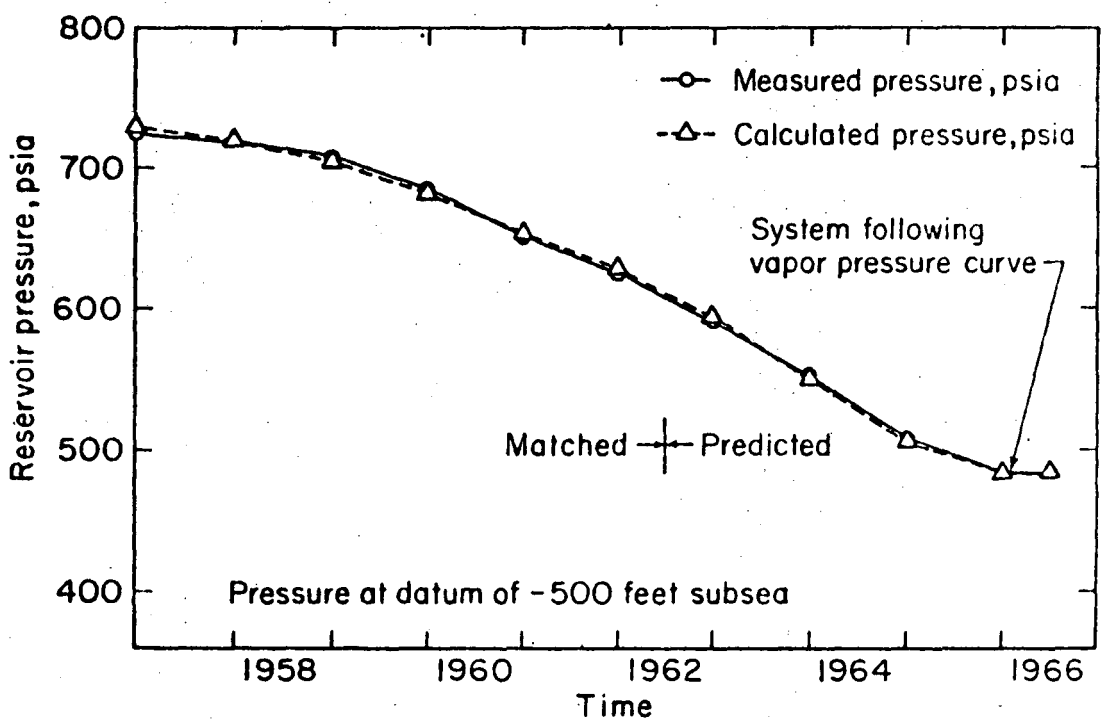

Fig. 16. Comparison of calculated with measured pressures for Wairakei geothermal system (after Whiting and Ramey, 1969).

The volume V can be expressed as

$$V\phi = M_o \left[S_o^G v_o^G + (1-S_o^G)\, v_o^L\right] = M_c \left[S_c^G v_c^G + (1-S_c^G)\, v_c^L\right] \tag{37}$$

where S^G is vapor (gas) saturation and v^G and v^L are specific volumes of vapor and liquid, respectively. The phase diagram for water (see Fig. 1) indicates that in the particular case where the system contains only compressed liquid, the thermodynamic path of decreasing pressure due to production will be essentially isothermal and isoenthalpic. Equations 35-37 then lead to a mass-volumetric balance similar to that employed for petroleum production above the bubble-point,

$$M_o\,(v^L - v_o^L) + M_e\, v^L - (M_p + M_\ell)\, v^L = 0 \tag{38}$$

Additional working hypotheses made by Whiting and Ramey are that Q is negligibly small relative to other terms in (36) and that $h_p = h_\ell$ (i.e., the enthalpy of produced and lost fluid is the same).

The compressed liquid version of this lumped-parameter model was applied by Whiting and Ramey to the Wairakei geothermal system in New Zealand. The initial temperature and enthalpy were estimated from field data, and a least-square fit to the production history from 1956 to 1961 was used to determine the initial water in place and the initial pressure. The model was then used to predict performance through 1965 and agreement with measured data was excellent (see Fig. 16). Prediction of future performance from 1966 to the year 2000 took into account two-phase conditions and indicated that pressure and temperature would decrease very little during this period. Recent field data from Wairakei have shown this prediction to be incorrect. The model was also used by Cady (1969) to simulate a laboratory setup but had to be applied separately to the two-phase and dry steam regions that developed.

Brigham and Morrow (1974) have adapted the lumped-parameter approach to vapor-dominated systems (i.e., systems with a significant dry steam region) by considering three different distributions of vapor and liquid. In each case

the system is assumed to be completely closed (i.e., the boundaries are impermeable and adiabatic) and energy is derived only from the rock mass itself.

Their first model concerns a single-phase system completely saturated with vapor. They assume that since the heat capacity of solid rock is much greater than that of steam, the system is essentially isothermal. Thus, there is no need for an energy equation and one can use a mass balance approach similar to that commonly employed in natural gas reservoirs. This approach leads to a linear relationship between p/Z and cumulative production ΔM^G according to the equation of state for a real gas,

$$\frac{p_1}{Z_1} = \frac{p_o}{Z_o}\frac{M_1^G}{M_o^G} = \frac{p_o}{Z_o}\left(\frac{M_o^G - \Delta M^G}{M_o^G}\right) \tag{39}$$

where Z is compressibility factor, M^G is mass of steam in place, and the subscripts indicate different values of time. The intercept of this line on the abscissa is equal to the original fluid in place, M_o^G.

In the second model the vapor phase is separated from an underlying layer of liquid by a horizontal interface at which boiling takes place. Since the vapor phase is again assumed to be isothermal, its treatment is similar to that in the previous model. The liquid phase changes its volume continuously and the corresponding lumped system is therefore defined as the pore space filled with liquid at the beginning of each pressure decrement. For this system the mass balance is simply

$$\Delta M^G = -\Delta M^L \tag{40}$$

whereas the energy balance for the fluid is expressed as

$$\underbrace{M_1^L e_1^L + M_1^G \bar{e}^G - M_o^L e_o^L}_{\text{Internal energy change}} = \underbrace{M_1^S c_p^S \left(T_o - T_1\right)}_{\text{Heat transferred from rock to liquid}}$$

$$+ \underbrace{\left(M_o^S - M_1^S\right) c_p^R \left(T_o - \frac{T_o + T_1}{2}\right)}_{\text{Heat transferred from rock to steam}} - \underbrace{\left(M_o^L - M_1^L - M_1^G\right)\bar{h}^G}_{\text{Enthalpy of vapor leaving system}} \tag{41}$$

where M^S is mass of rock in contact with liquid, $\bar{h}^G$ is average enthalpy of vapor leaving system and $\bar{e}^G$ is average internal energy of vapor (both calculated at the average temperature $(T_o + T_1)/2$) and the subscripts o and 1 indicate the beginning and end of a depletion step, respectively. Brigham and Morrow further simplified this equation by reformulating it in terms of enthalpy and neglecting the resulting pressure terms and obtained

$$M_1^L h_1^L - M_o^L h_o^L = M_1^S c_p^S \left(T_o - T_1\right) + \left(M_o^S - M_1^S\right) c_p^S \left(\frac{T_o - T_1}{2}\right) - \left(M_o^L - M_1^L\right) \bar{h}^G \qquad (42)$$

Given a rate of production, the resulting system of nonlinear equations can be solved in an iterative manner.

The third model considers a vapor phase overlying a layer of liquid except that now boiling occurs throughout the entire thickness of this layer and its depth remains fixed in time. The resulting energy equation is essentially similar to that of Whiting and Ramey (1969) with the exception that only steam is allowed to leave the system.

Application of these models to various hypothetical reservoirs has shown that in estimating available reserves by extrapolation of early p/Z behavior, the results will tend to be optimistic when porosity is low, but pessimistic when porosity is high. The constant liquid level model was found to predict higher recovery for a given pressure depletion than the falling liquid level model. The presence of even a small amount of liquid in the lower part of a geothermal system was shown to be extremely important because it can account for a large fraction of the total fluid mass and can significantly affect the results of a p/Z analysis. Finally, Brigham and Morrow conclude that "the steam portion of a reservoir will always remain isothermal whether or not there is boiling water below the steam. Thus pressure, temperature, and enthalpy measurements will not be completely diagnostic for determining the original state of the reservoir

fluid system. Because the steam remains essentially isothermal, it gradually increases in enthalpy and becomes superheated as the pressure declines."

An interesting lumped-parameter model based on the assumption that the liquid and gas phases are uniformly distributed throughout the system has been proposed recently by Martin (1975). The system is assumed to be completely closed and each phase is produced at a rate which is related to its relative permeability. His approach is based on a simplified form of equations 1-3 and 6. If we neglect the gravity term in Darcy's law and substitute (2) and (3) into (1), we can write for an isotropic medium

$$\frac{\partial}{\partial x_i}\left(\lambda^f \frac{\partial p}{\partial x_i}\right) = \frac{\partial M^f}{\partial t} \tag{43}$$

where

$$\lambda^f = k\left(\frac{\rho^L k_r^L}{\mu^L} + \frac{\rho^G k_r^G}{\mu^G}\right)$$

$$M^f = \phi\,(\rho^L S^L + \rho^G S^G)$$

Neglecting heat dispersion and the pressure terms in (6) we obtain by the same procedure

$$\frac{\partial}{\partial x_i}\left(\lambda^h \frac{\partial p}{\partial x_i}\right) = \frac{\partial M^h}{\partial t} \tag{44}$$

where

$$\lambda^h = \frac{\rho^L h^L k k_r^L}{\mu^L} + \frac{\rho^G h^G k k_r^G}{\mu^G} + \kappa^{eff}\frac{dT}{dp}$$

$$M^h = \phi S^L \rho^L h^L + \phi S^G \rho^G h^G + (1-\phi)\rho^S c_v^S T$$

since T and p are uniquely related by the boiling curve. The notion of a lumped-parameter model implies that gradients of pressure, temperature, and saturation are small. Expanding (43) and (44) and neglecting the products of these gradients leads to

$$\frac{1}{\lambda^f}\frac{\partial M^f}{\partial t} = \frac{\partial^2 p}{\partial x_i^2} = \frac{1}{\lambda^h}\frac{\partial M^h}{\partial t} \tag{45}$$

Expanding the time derivatives with respect to p and S yields the nonlinear ordinary differential equation

$$\frac{dS^L}{dp} = \frac{\lambda^h \frac{\partial M^f}{\partial p} - \lambda^f \frac{\partial M^h}{\partial p}}{\lambda^f \frac{\partial M^h}{\partial S^L} - \lambda^h \frac{\partial M^f}{\partial S^L}} \tag{46}$$

In the case of single-phase flow, T and p are not related uniquely to each other, and the above procedure must therefore be modified. If we neglect heat conduction as well as dispersion, we obtain the single-phase equivalent of (45) with $\lambda^h = h\lambda^f$. Expanding the time derivatives with respect to p and T leads to the following nonlinear ordinary differential equation,

$$\frac{dT}{dp} = \frac{\frac{\partial M^h}{\partial p} - h \frac{\partial M^f}{\partial p}}{h \frac{\partial M^f}{\partial T} - \frac{\partial M^h}{\partial T}} \tag{47}$$

Equations 46 and 47 were used by Martin to calculate numerically the relationships between T, p and S in a hypothetical system free of gravity effects. Integration of (47) showed that in the case of a single phase, dT/dp is very small and the exploitation process is essentially isothermal. This is clearly illustrated in Fig. 17 which shows the thermodynamic paths for various initial p-T conditions in a system with $\phi = 0.25$, $\rho^S = 162$ lb/ft^3 (2.6 gm/cm^3), $c_v^S = 0.2$ Btu/lb ^oF (0.2 cal/gm ^oC), $\kappa^{eff} = 40$ Btu/ft day ^oF (0.0069 cal/cm sec ^oC), k = 1 darcy (9.87×10^{-9} cm^2), and typical k_r values. For example, from initial conditions corresponding to point A, the temperature will drop slightly along line 1 as pressure declines. This corresponds to a single phase (essentially steam) reservoir with temperature and pressure above the critical point. However, if the system is initially saturated with liquid water at point C, production causes an isothermal decrease in pressure until the boiling curve is reached. At this stage p and T begin to follow the boiling curve with a gradual increase in steam saturation. Production of

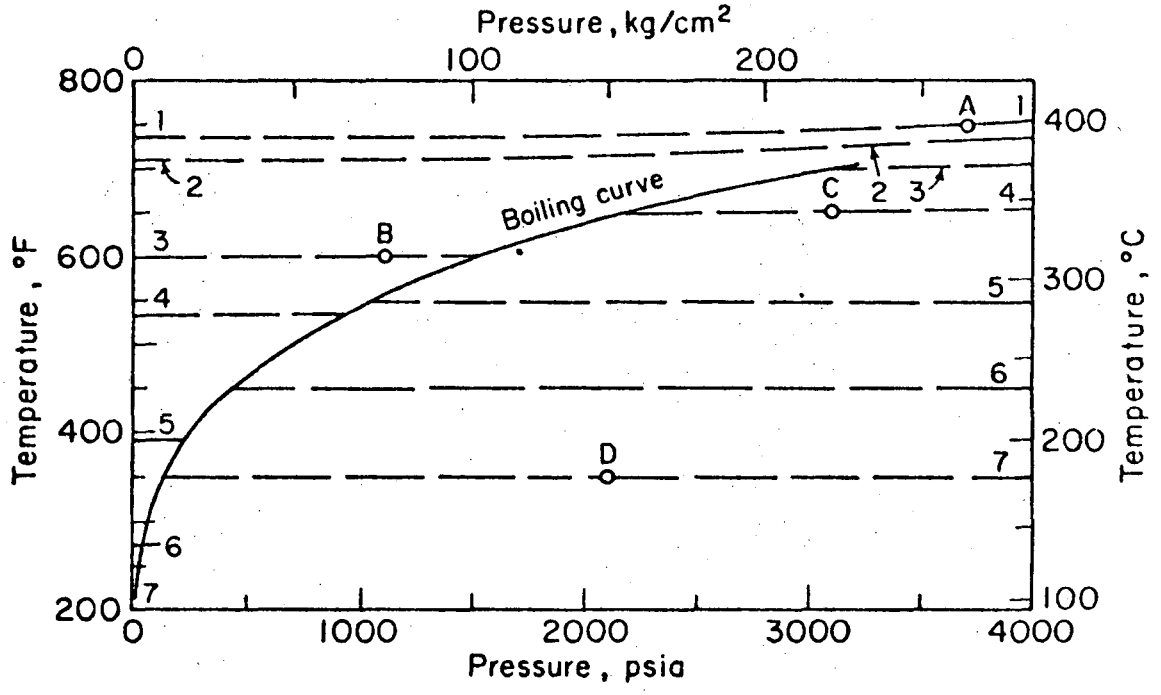

Fig. 17. Pressure-temperature diagram for pure water and vapor showing various thermodynamic paths for depleting a geothermal system (after Martin, 1975).

steam, however, starts only when S^G reaches its so-called equilibrium value at which the vapor phase becomes mobile (below this value $k_r^G = 0$). The ratio between produced steam and liquid water continues to increase until S^L is reduced to a stage where the liquid becomes immobile and production is restricted to saturated steam. When all the water has been boiled away and $S^L = 0$, the temperature departs from the boiling curve and superheated steam is produced under essentially isothermal conditions.

From his study Martin further concluded that "under certain conditions only a relatively small amount of the heat initially contained in a geothermal reservoir will be produced during pressure depletion. Much of this heat may be contained in the produced steam even though initially the reservoir contains only hot water." This is due to the higher heat content and lower viscosity of steam as compared with liquid water. A similar reasoning also led Martin to conclude that "for many conditions where gravity segregation of the steam and hot water occurs during depletion, more of the total heat can be produced by completing wells high in the reservoir to enhance steam production and suppress water production." When gravity effects are important, system C should follow the path shown in Fig. 17 until the steam phase becomes mobile and gravity segregation begins. Since S^G increases rapidly in the upper portion of the system, departure from the boiling curve will occur at considerably higher p and T values than is shown in the figure. In the lower portion of the system S^L decreases slowly and therefore departure from the boiling curve will occur at lower p and T values than in Fig. 17.

Distributed-Parameter Models

A model in which the properties of the rock and/or the fluid (e.g., saturation, viscosity, pressure, etc.) are allowed to vary in space will be called a distributed-parameter model. By taking into account spatial variations of these properties the resulting problem may become too complex to be treated analytically.

An alternative approach is to replace the governing partial differential equations by an equivalent set of algebraic equations and then solve the problem numerically with the aid of a computer. The purpose of the following discussion is to acquaint the reader with some of the results obtained to date by numerical simulation of relatively complex geothermal systems.

A considerable degree of sophistication in the numerical simulation of immiscible, multiphase and multicomponent fluid flow problems under nonisothermal conditions has been achieved in recent years by petroleum engineers. A brief review of this work has been included in a recent paper by Coats et al. (1974). Most of this effort, however, was not concerned with geothermal systems but was directed toward the problem of oil recovery by steamflooding, hot waterflooding, steam stimulation, and other thermal processes which are of immediate concern to the petroleum industry. For example, Spillette and Nielsen (1968) have studied the response of an oil reservoir to hot water injection by assuming that the hydrocarbons and the water will appear only as a liquid phase. Their model consists of a vertical cross-section including a horizontal layer of sand enclosed between two impermeable shale strata. Energy is transported by conduction and convection in the sand layer and by conduction in the shale layers. Fluid densities and viscosities are taken to be temperature dependent and capillary pressure between the two fluid components is taken into account. The equations governing mass transport are solved by an alternating direction implicit (ADI) iterative finite difference procedure whereas the energy equation is solved by the method of characteristics. One of the conclusions of this study was that fluid segregation due to gravity has a significant effect on the system considered.

Another two-dimensional vertical model consisting of a sand layer sandwiched between two impermeable strata has been developed more recently by Weinstein et al. (1974). In this model fluid flow is allowed to take place only in one horizontal direction whereas energy may be transferred by conduction both

horizontally and vertically through the entire system. However, the hydrocarbons and water can coexist both in the liquid and vapor states, so that one must now deal with three distinct phases: oil, water, and gas. The gas phase is a mixture of steam and hydrocarbon vapor. Interphase mass transfer within each component is allowed to account for processes such as water vaporization, steam condensation, hydrocarbon distillation, solvent extraction, and solution-gas drive. The energy equation is expressed in terms of enthalpy, rock compressibility is taken into account, but capillary pressure effects are neglected. A finite difference approach is employed with an implicit pressure-explicit saturation formulation of the mass balance equation, which is solved simultaneously with the energy equation. The authors also discuss various improved numerical techniques for invoking phase constraints and calculating mass transfer terms.

A three-dimensional finite difference model describing nonisothermal, three-phase flow of oil, liquid water, and steam has been described by Coats et al. (1974) for the purpose of simulating oil recovery by steam and hot water injection. In this model fluid densities are taken to be linear functions of temperature and pressure, and the effect of pressure on porosity is also taken into account. The mass and energy balance equations are solved simultaneously by a direct method. A comparison of calculated results with experimental data indicated that the simulation process is sensitive to temperature effects on relative permeability. The authors concluded that such data, especially the temperature dependence of water relative permeabilities, must be taken into account.

The first application of a distributed-parameter model to a geothermal system was made by Mercer (1973) and Mercer and Pinder (1974). A comprehensive account of this work has been described more recently by Mercer et al. (1975). The model consists of a single-phase, two-dimensional areal (horizontal) representation of the hot-water Waiora aquifer in the Wairakei hydrothermal system of New Zealand. The mass and energy balance (Eq. 7 without the pressure term)

are solved in the horizontal plane of the aquifer by the Galerkin finite element approach, using isoparametric elements as shown in Fig. 18. Since the governing equations are averaged over the thickness of the aquifer, cellular convection does not play a role in the resulting model.

However, vertical flow of fluid as well as energy is allowed to take place between the Waiora formation and the overlying Wairakei breccia aquifer through the intervening Huka Falls shale (see Fig. 19). The rate of this vertical leakage is taken to be proportional to the differences in head and temperature between the two aquifers, the values of p and T in the upper aquifer being kept constant. Inflows of heat from the underlying ignimbrites into the Waiora aquifer are treated as unknown source terms to be determined by model calibration. The lateral boundaries of the Waiora aquifer are assumed to be impermeable and isothermal. Viscosity is allowed to vary with temperature whereas fluid density is calculated as a linear function of temperature and pressure. The model is also capable of treating the heat dispersion term in its proper tensorial form.

The first step in applying the model to Wairakei was to adjust the parameters so as to reproduce the steady state conditions existing in 1955, prior to exploitation. The parameters that were adjusted at this stage included element configuration, heat sources at the bottom of the aquifer, dispersion coefficients, and permeabilities. A sensitivity analysis was performed indicating that dispersion had little influence on the results, whereas the permeability of the Huka Falls formation had an important effect on the temperature distribution in the thermal reservoir.

The second step was to simulate the response of the geothermal field to withdrawal of hot water from a series of wells during the period between 1955 and 1962, using time steps of 30 days. The parameters of the model were again adjusted so as to bring about a fit between calculated and observed data. The results showed only a slight change in the configuration of the isotherms during

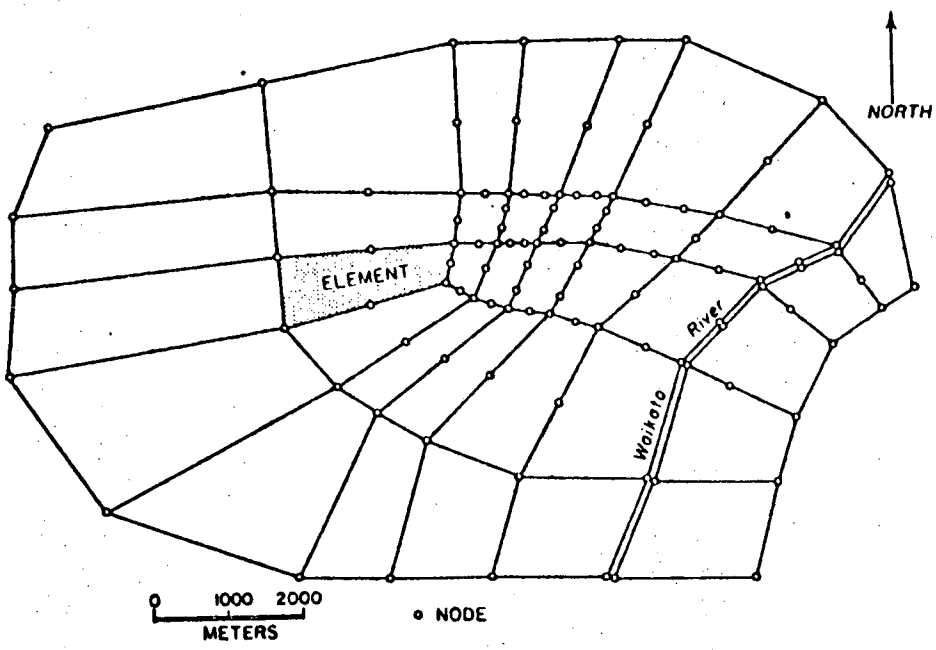

Fig. 18. Network of isoparametric elements used in distributed-parameter model of Wairakei geothermal system (after Mercer et al., 1975).

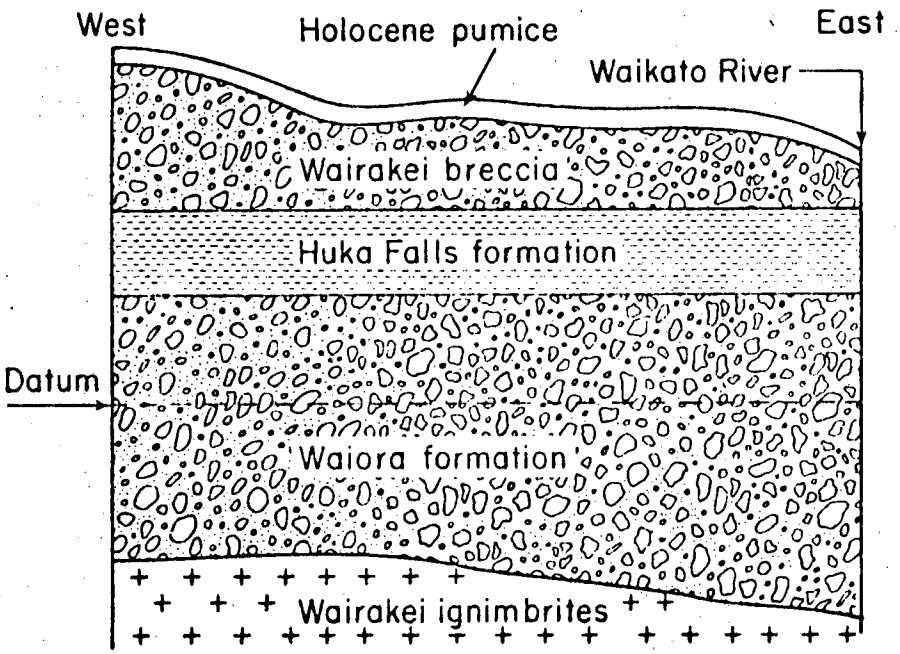

Fig. 19. Generalized geologic cross-section of Wairakei geothermal system. Datum plane 152.4 m above sea level (after Mercer et al., 1975).

the period investigated. Fig. 20 is a comparison of computed and observed potentiometric surfaces in the Waiora aquifer for 1958 and 1962. The single-phase model failed to reproduce historical data after the calibration period of 1955-1962 due to a considerable quantity of steam that had formed in the Waiora aquifer as a result of exploitation. Faust and Mercer (1975) are now developing a two-phase model to handle such problems.

A two-dimensional model of transient single-component, two-phase flow in a geothermal system has been developed by Toronyi (1974). The model is based on Equations 1-3 and 6 (without the last two terms involving pressure) and utilizes a block-centered rectangular finite difference grid capable of simulating flow in either a horizontal or vertical plane. The resulting equations are expressed in an implicit backward difference form and are solved simultaneously by a line iterative quasi-linearization (Newton-Raphson) scheme. Anisotropy is taken into account with the restriction that principal permeabilities and heat conductivities must remain parallel to the coordinates. Thermal conductivity is calculated according to (5) but dispersion is not taken into account. The fluids are assumed to have temperatures and pressures that are always on the vapor pressure curve implying that liquid and vapor co-exist at every point in the system. Consequently p and S are the two dependent variables for which a solution is sought simultaneously.

The external boundaries are impermeable and adiabatic with the understanding that forced convection due to production is much greater than conduction across these boundaries. The distributed-parameter model is coupled to a one-dimensional steady state model of a producing well in which the fluid is assumed to form a homogeneous two-phase mixture. The well is treated as a point source in the finite difference model which, in turn, provides boundary values of p and S for the steady state wellbore model. The wellbore model is represented mathematically by first order ordinary differential equations which are solved by the Runge-Kutta method.

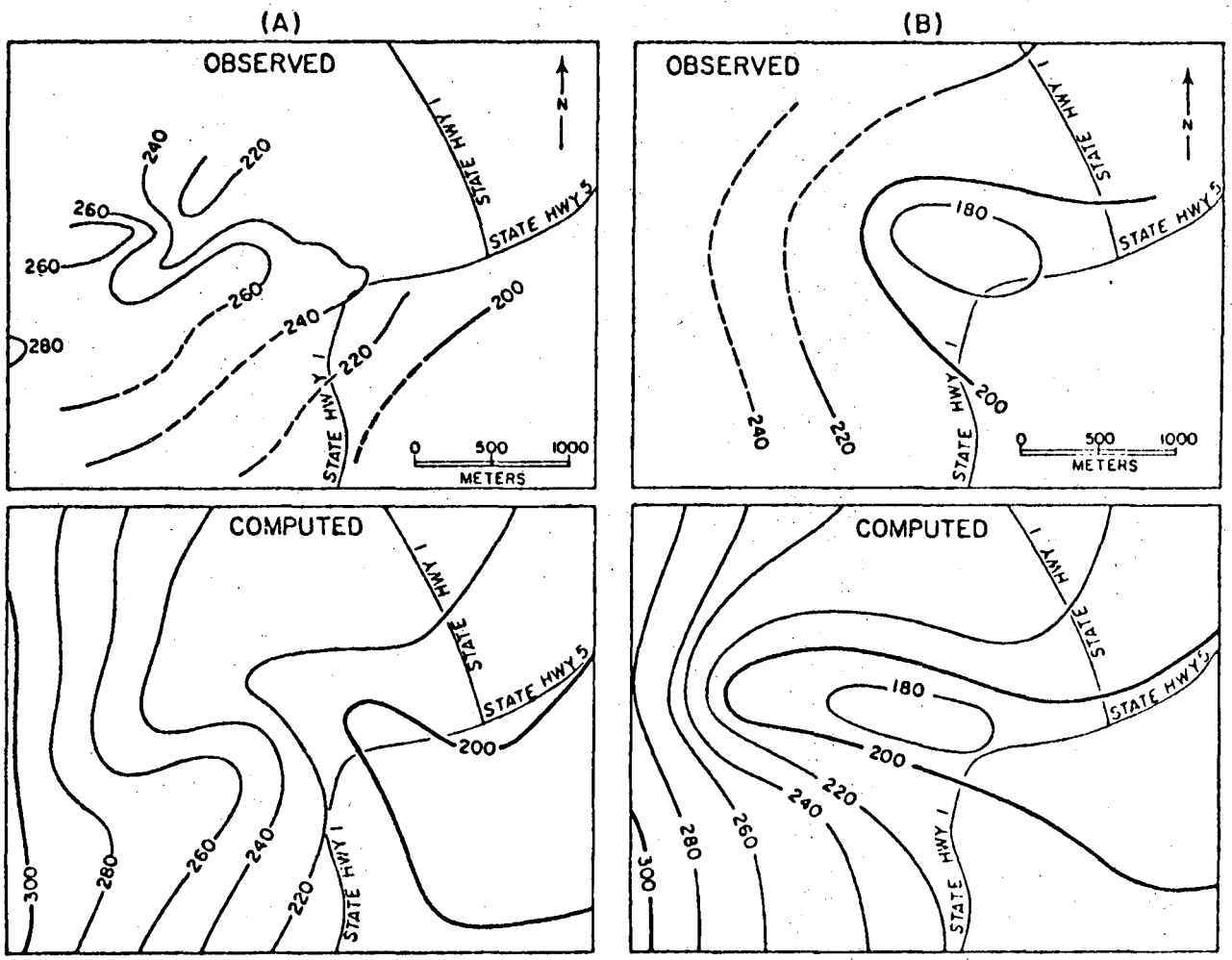

Fig. 20. Comparison of computed with observed potentiometric surfaces in Waiora hot-water aquifer for (A) 1958 and (B) 1962. Values in meters from datum 152.4 m above sea level (after Mercer et al., 1975).

Toronyi applied his model only to a homogeneous and isotropic geothermal system by using a 6 x 6 rectangular finite difference grid. His purpose was to investigate the effects of porosity, permeability, and various uniform initial p and S distributions on the production of geothermal fluid in a horizontal and vertical plane. On the basis of these studies, Toronyi classified the behavior of two-phase geothermal systems into three types in terms of initial liquid saturation: (1) vapor dominated, with initial $S^L < 40\%$; (2) liquid dominated, with initial $S^L > 60\%$, and (3) mixed or intermediate, with initial S^L within the range 40 - 60%. Condensation and vaporization were found to be very important phenomena that could create exceedingly high liquid saturations near a wellbore and disrupt gravitational equilibrium by causing more liquid to occur at the top of the system than at the bottom. Toronyi also found that superheated regions form faster in rocks having relatively low porosity and permeability values. The quality of the produced fluid (in terms of percent steam) was always found to be greater at the wellhead than at the bottom, although the maximum change in quality was small.

A two-phase, multi-dimensional model for geothermal systems has recently been developed by Lasseter et al. (1975) based on an extension of an earlier investigation of single-phase flow under noniosthermal conditions (Lasseter and Witherspoon, 1974). This model utilizes Equations 1 through 4. In the numerical process, Equations 1 through 3 are combined into a flow equation which is then solved in conjunction with the energy equation (Eq. 4). These two equations expressed in an integrated finite difference form (Narasimhan and Witherspoon, 1975) are solved for the two dependent variables, density and energy of the fluids, as a function of time and position within the system. Advantage can be taken of the fact that the time constants for the energy equation are typically several orders of magnitude larger than the time constants of the flow equation, which permits one to decouple the governing equations and still handle the

non-linearities satisfactorily. Thus, while it is necessary to take relatively small time steps to accurately solve the flow equation, the energy field time steps can be much larger.

Some preliminary results for a model of a vapor-dominated geothermal system are shown in Fig. 21. A vertical cross-section of a cylindrical system with a height of 3000 m and a radius of 2000 m was set up using 150 elements. The vapor column had an average initial temperature and pressure of 250°C and 40 kg/cm^2 throughout, and an attempt was also made to simulate a 200 m bottom layer that was essentially liquid saturated. The lower boundary of the boiling water layer was maintained at 250°C while the other boundaries were arbitrarily made impermeable to both heat and fluid. Typical values for thermal and flow properties of the materials were assumed. Relative permeability data were temperature independent.

Figure 21 shows reproductions of computer plots after about 1500 days at a steam withdrawal rate from the producing interval of 3×10^7 kg/day (1380 t/h). As a result of this high rate of production, the pressure in the vapor column dropped to about 25 kg/cm^2 (Fig. 21A) and the temperature decreased to about 225°C (Fig. 21B). Figure 21C is a vector plot of the vapor flux showing how vigorous boiling at the bottom of the system is producing substantial steam. Figure 21D is a vector plot of the liquid flux and shows how water is separating from the steam at the base of the system. These preliminary results serve to illustrate the power of this numerical approach in analyzing such complex systems.

Gringarten and Sauty (1975) have developed an analytical model for nonsteady temperature behavior of production wells during reinjection of heat-depleted water into a horizontal aquifer with uniform regional flow. The aquifer is of infinite lateral extent and is confined between two impermeable semi-infinite layers. Initially, the system has a uniform temperature, T_o. At time $t = 0$, a well starts producing water at rate Q and injection of relatively cold water starts in a second well in the same aquifer at the same rate. The temperature

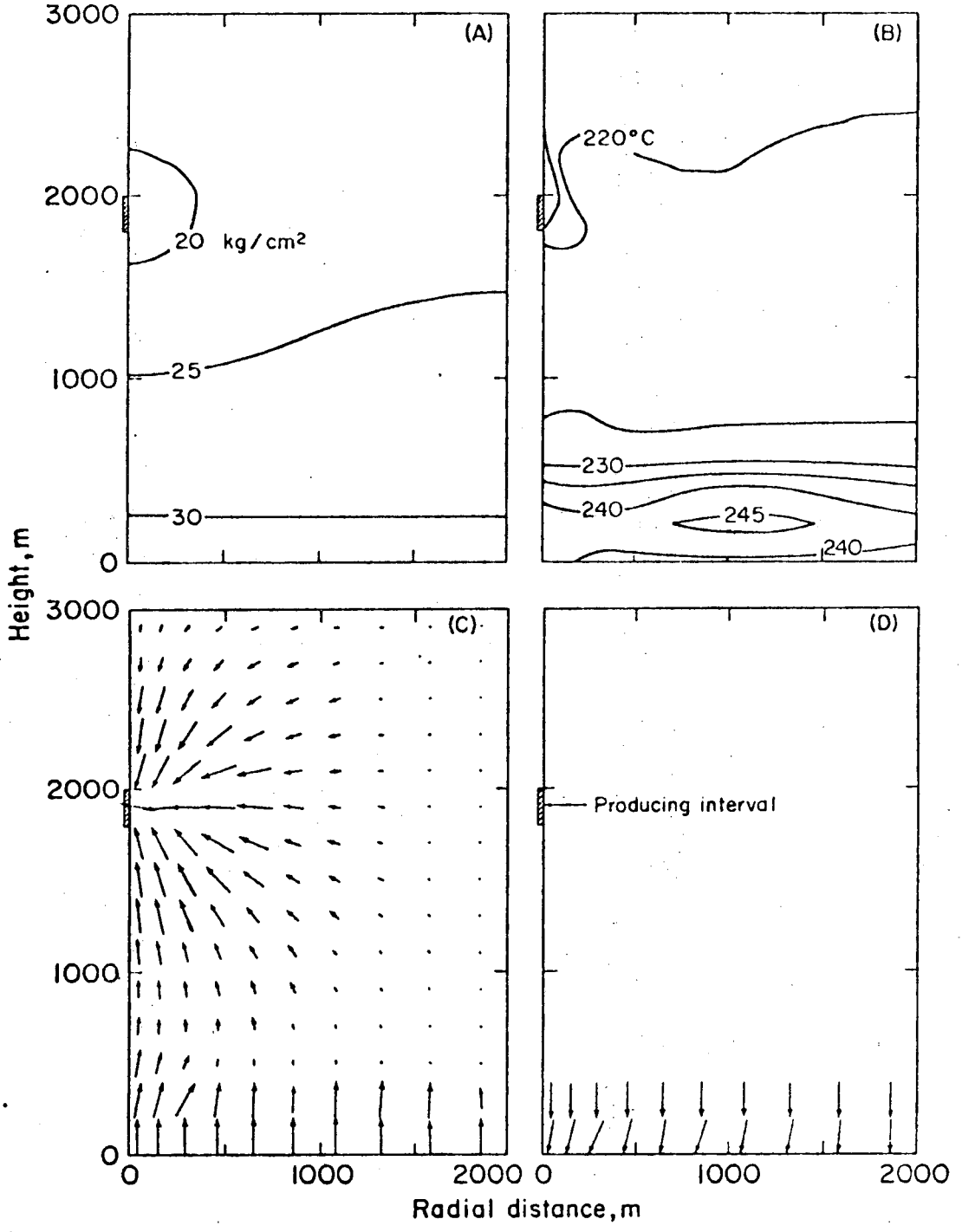

Fig. 21. Distributed-parameter model of vapor-dominated geothermal system showing reservoir conditions after 1500 days of production: (A) pressure field, (B) temperature field, (C) vapor flux, (D) liquid flux.

of the injected water is set equal to T_1 and maintained constant thereafter. Such a pair of wells is known as a "doublet."

The authors assume that steady state fluid flow is established much faster than thermal equilibrium and that temperature transfer occurs only by forced horizontal convection in the aquifer and vertical conduction in the confining beds. Assuming further that the waters at temperatures T_o and T_1 do not mix (piston displacement), they have arrived at a simple closed form mathematical relationship between temperature, certain dimensionless parameters, and the stream function characterizing water flow. Gringarten and Sauty used their solution to calculate the optimum spacing of isolated doublets to be drilled for space heating purposes in the 1800 m deep Dogger aquifer around Paris, under the requirement that the cold front does not reach the producing well in less than 30 years when Q = 100 m^3/h. By introducing a safety factor into their calculations, the optimum spacing was found to be about 900 m for an aquifer 50 m thick.

NOMENCLATURE

Symbol	Description	Dimensions
a, a_1, a_2	width	L
c_p	specific heat at constant pressure	$L^2t^{-2}T^{-1}$
c_v	specific heat at constant volume	$L^2t^{-2}T^{-1}$
D	depth	L
D_1, D_2	aspect ratio	-
D_{ij}	mechanical heat dispersion tensor	$MLt^{-3}T^{-1}$
e	specific internal energy	L^2t^{-2}
f	fluid property	arbitrary
g	acceleration due to gravity	Lt^{-2}
g_i	gravity vector (0, 0, -g)	Lt^{-2}

Symbol	Description	Dimensions
h	specific enthalpy	L^2t^{-2}
H	heat capacity ratio	-
k	intrinsic permeability	L^2
k_{ij}	intrinsic permeability tensor	L^2
k_r	relative permeability	-
L	length	L
m	specific mass flux	$ML^{-2}t^{-1}$
M	mass	M
n_i	outward unit normal vector on Γ	-
Nu	Nusselt number	-
p	pressure	$ML^{-1}t^{-2}$
p_D	dimensionless pressure	-
Pr	Prandtl number	-
q_i	specific conductive heat flux vector	Mt^{-3}
Q	heat flux	ML^2t^{-3}
r	radius	L
R	representative elementary volume	L^3
Ra	Rayleigh number	-
Ra_c	critical Rayleigh number	-
S	fluid saturation	-
t	time	t
T	temperature	T
v	specific volume	L^3M^{-1}
v_i	darcy velocity vector	LT^{-1}
V	volume	L^3
w_i	velocity vector of solid fluid interface	Lt^{-1}

Symbol	Description	Dimensions
x_i	vector of space coordinates (x,y,z) z being the vertical	L
Z	compressibility factor for real gas	-
α	thermal diffusivity	L^2t^{-1}
β	coefficient of volumetric thermal expansion	T^{-1}
Γ^{LS}	liquid-solid interface in R	L^2
Γ^{LG}	liquid-gas interface in R	L^2
Γ^{GS}	gas-solid interface in R	L^2
δ_{ij}	kronecker delta (1 if i = j and 0 if i ≠ j)	-
θ	dimensionless temperature	-
κ	thermal conductivity	$MLt^{-3}T^{-1}$
κ_{ij}	thermal dispersion tensor	$MLt^{-3}T^{-1}$
μ	viscosity	$ML^{-1}t^{-1}$
ν_i	dimensionless velocity vector	-
ρ	density	ML^{-3}
τ	dimensionless time	-
ϕ	porosity	-
$< >$	average over R	arbitrary
$< >^*$	average over pore space of R	arbitrary
$< >^{L,G,S}$	average over liquid, gas, or solid phases in R	arbitrary
Subscripts		
o	reference quantity	
Superscripts		
eff	effective quantity for fluid-filled rock	
G	gas phase	

Symbol	Description	Dimensions
L	liquid phase	
S	solid phase	
o	deviation from average over R	

ACKNOWLEDGMENTS

We would like to acknowledge the support for this work provided by the U. S. Atomic Energy Commission, the U. S. Geological Survey, and the University of California.

APPENDIX

The purpose of this appendix is to derive a macroscopic form of the energy balance equation for a two-phase, single component fluid in a porous medium. This is accomplished by averaging the microscopic equations over a representative elementary volume (Bear, 1972, p. 19) of the medium. The particular method of averaging that is used here has been applied by Lee et al. (1975) to the energy equation and, in this context, was brought to our attention by Gray and Pinder (1974, personal communication). We recognize that the macroscopic energy equation can be derived directly from macroscopic balance considerations, without resorting to an averaging process. However, the formal averaging procedure is helpful in gaining insight into the numerous assumptions that one must make in order to arrive at a manageable macroscopic expression. Such assumptions are implicitly inherent in every macroscopic equation and, by facing them explicitly, one should be able to appreciate some of the limitations of the differential equations used to describe geothermal systems.

Mathematical Preliminaries

Let R be a representative elementary volume of the porous medium and let ϕ be the porosity of R. Whitaker (1969) demonstrated that the averaging procedure used below will lead to meaningful results if the characteristic length of R is much greater than the characteristic length of the pores, and is much smaller than the characteristic length of the entire porous medium. An obvious requirement is that R be large enough to provide a fair representation of all the statistical properties of the pore space. Our analysis is restricted to homogeneous porous media which means that the porosity, ϕ, as well as all other statistical properties of the pore space, must remain unchanged as one focuses his attention on different elementary representative volumes in the medium. Furthermore, the size and shape of R must be constant and its orientation must remain unchanged.

Let $f^L(x_1)$ be some property of the liquid (e.g., density, temperature, etc.) which, by definition, is zero in the gas phase and in the solids. Then the "liquid phase average" of f^L is defined as

$$\langle f^L \rangle^L = \frac{1}{\phi S^L R} \int_R f^L \, dR \tag{A1}$$

Similarly, the "pore volume average" of f^L is defined as

$$\langle f^L \rangle^* = \frac{1}{\phi R} \int_R f^L \, dR \tag{A2}$$

and the "bulk volume average" as

$$\langle f^L \rangle = \frac{1}{R} \int_R f^L \, dR \tag{A3}$$

From (A1) - (A3) it is evident that

$$\langle f^L \rangle = \phi \langle f^L \rangle^* = \phi S^L \langle f^L \rangle^L \tag{A4}$$

These averages can be viewed as point macroscopic quantities associated with the centroid of R. Thus, there is an average associated with each point in R (each such point being the centroid of another R), and it therefore makes sense to talk about the average value of these averages over R. Whitaker (1969) showed that

$$\langle\langle f^L \rangle\rangle = \langle f^L \rangle \tag{A5}$$

i.e., the average of the average is equal to the average (note that this is by no means self evident).

At any point in the liquid phase within R, f^L can be expressed as

$$f^L = \langle f^L \rangle^L + \overset{\circ}{f}{}^L \tag{A6}$$

where $\overset{\circ}{f}{}^L$ is simply the deviation from the phase average of f^L. From (A5) and (A6) it follows that

$$\langle \overset{\circ}{f}{}^{L} \rangle^{L} \equiv 0 \tag{A7}$$

Note that just like f^L, the function of $\overset{\circ}{f}{}^{L}$ is taken to be zero everywhere outside the liquid phase.

According to the general transport theorem (c.f. Whitaker, 1968) one has

$$\langle \frac{\partial f^L}{\partial t} \rangle = \frac{\partial \langle f^L \rangle}{\partial t_i} - \frac{1}{R} \int_{\Gamma^{LS}, \Gamma^{LG}} f^L w_i n_i \, d\Gamma \tag{A8}$$

where n_i is a unit normal pointing out of the liquid phase. Another useful relationship known as the "averaging theorem" (Whitaker, 1969; Slattery, 1972, pp. 192-196) states that

$$\langle \frac{\partial f^L}{\partial x_i} \rangle = \frac{\partial \langle f^L \rangle}{\partial x_i} + \frac{1}{R} \int_{\Gamma^{LS}, \Gamma^{LG}} f^L n_i \, d\Gamma \tag{A9}$$

Similar relationships will hold for properties of the solid phase, f^S, and the gas phase, f^G.

Derivation of Energy Equation for Two-Phase Fluid

In the following analysis, the pore space is assumed to be saturated by a single-component fluid which can be either in a liquid or gaseous state. The liquid and gas phases are assumed to be separated by a distinct interface, Γ^{LG}, across which there may be a finite change in pressure. If one neglects viscous dissipation, then the energy equation at a point within the liquid can be written (c.f., Currie, 1974, p. 17) as

$$\frac{\partial}{\partial t} (\rho^L e^L) = - \frac{\partial}{\partial x_i} (\rho^L e^L v_i{}^L) - p^L \frac{\partial v_i{}^L}{\partial x_i} - \frac{\partial q_i{}^L}{\partial x_i} \tag{A10}$$

Taking the average of (A10) over a representative elementary volume, R, and using (A8) and (A9), the result (after rearrangement) is

$$\frac{\partial}{\partial t}\langle \rho^L e^L \rangle = -\frac{\partial}{\partial x_i}\langle \rho^L e^L v_i^L \rangle - \frac{1}{R}\int_{\Gamma^{LG}} \rho^L e^L (v_i^L - w_i)\, n_i \, d\Gamma$$

$$- \phi S^L \langle p^L \rangle^L \frac{\partial \langle v_i^L \rangle^L}{\partial x_i} - S^L \langle p^L \rangle^L \frac{1}{R}\int_{\Gamma^{LG}} v_i^L \, n_i \, d\Gamma$$

$$- \frac{\partial \langle q_i^L \rangle}{\partial x_i} - \frac{1}{R}\int_{\Gamma^{LS},\Gamma^{LG}} q_i^L \, n_i \, d\Gamma \qquad \text{(A11)}$$

Equation A11 is based on the assumption that fluid velocity normal to a solid-fluid interface is zero (i.e., there is no transfer of kinetic energy between the fluid and the solid). Furthermore, in order to replace the term $p^L(\partial v_i^L/\partial x_i)$ in (A10) by its macroscopic equivalent in (A11), it is necessary to assume that $\overset{\circ}{p}{}^L$ and $\partial \overset{\circ}{v}{}_i^L/\partial x_i$ are uncorrelated so that the average of their product is zero. A possible physical justification for this is to say that local variations in fluid velocity within a pore are controlled primarily by viscous stresses and can therefore be assumed to be independent of pressure.

The energy equation for the gas phase at a point within R has the same form as (A11). When this equation is averaged over R, the result is

$$\frac{\partial}{\partial t}\langle \rho^G e^G \rangle = -\frac{\partial}{\partial x_i}\langle \rho^G e^G v_i^G \rangle + \frac{1}{R}\int_{\Gamma^{LG}} \rho^G e^G (v_i^G - w_i)\, n_i \, d\Gamma$$

$$- \phi S^G \langle p^G \rangle^G \frac{\partial \langle v_i^G \rangle^G}{\partial x_i} + S^G \langle p^G \rangle^G \frac{1}{R}\int_{\Gamma^{LG}} v_i^G n_i \, d\Gamma$$

$$- \frac{\partial \langle q_i^G \rangle}{\partial x_i} - \frac{1}{R}\int_{\Gamma^{GS}} q_i^G \, n_i \, d\Gamma + \frac{1}{R}\int_{\Gamma^{LG}} q_i^G \, n_i \, d\Gamma \qquad \text{(A12)}$$

Here n_i points into the gas along Γ^{LG} and into the solid along Γ^{GS}.

The energy equation at a point within the solid is simply

$$\frac{\partial}{\partial t}(\rho^S e^S) = -\frac{\partial q_i^S}{\partial x_i} \tag{A13}$$

Integrating over R gives

$$\rho^S \frac{\partial \langle e^S \rangle}{\partial t} = -\frac{\partial \langle q_i^S \rangle}{\partial x_i} + \frac{1}{R}\int_{\Gamma^{LS},\Gamma^{GS}} q_i^S n_i \, d\Gamma \tag{A14}$$

where n_i points into the solid.

From the requirement of energy continuity at a liquid-gas interface, it can be shown that

$$\int_{\Gamma^{LG}} [q_i^L + \rho^L e^L (v_i^L - w_i)] n_i d\Gamma = \int_{\Gamma^{LG}} [q_i^G + \rho^G e^G (v_i^G - w_i)] n_i d\Gamma \tag{A15}$$

A similar condition must also hold for the conductive energy flux $q_i n_i$ at any solid-fluid interface. Thus, by adding (A11), (A12), and (A14) and using (A4) we obtain

$$\begin{aligned}
&\frac{\partial}{\partial t}[\phi S^L \langle \rho^L e^L \rangle^L + \phi S^G \langle \rho^G e^G \rangle^G + (1-\phi)\rho^S \langle e^S \rangle^S] \\
&= -\frac{\partial}{\partial x_i}[\phi S^L \langle \rho^L e^L v_i^L \rangle^L + \phi S^G \langle \rho^G e^G v_i^G \rangle^G] \\
&- \frac{\partial}{\partial x_i}[\phi S^L \langle q_i^L \rangle^L + \phi S^G \langle q_i^G \rangle^G + (1-\phi)\langle q_i^S \rangle^S] \\
&- \phi S^L \langle p^L \rangle^L \frac{\partial \langle v_i^L \rangle^L}{\partial x_i} - \phi S^G \langle p^G \rangle^G \frac{\partial \langle v_i^G \rangle^G}{\partial x_i} \\
&- S^L \langle p^L \rangle^L \frac{1}{R}\int_{\Gamma^{LG}} v_i^L n_i \, d\Gamma + S^G \langle p^G \rangle^G \frac{1}{R}\int_{\Gamma^{LG}} v_i^G n_i \, d\Gamma
\end{aligned} \tag{A16}$$

We now introduce another assumption that thermodynamic relationships between average (macroscopic) quantities remain exactly the same as those between the equivalent point (microscopic) quantities. This assumption is implicit in all macroscopic equations that we have encountered in the literature. Its implication is that $\dot{\rho}$ and $\dot{e}$ are uncorrelated and one can thus replace $\langle \rho^L e^L \rangle^L$ by $\langle \rho^L \rangle^L \langle e^L \rangle^L$ and $\langle \rho^G e^G \rangle^G$ by $\langle \rho^G \rangle^G \langle e^G \rangle^G$. Since mass dispersion is not considered in the

present analysis, $\overset{\circ}{\rho}$ and $\overset{\circ}{v}_i$ are also uncorrelated and we can therefore write

$$\phi S^L \langle \rho^L e^L v_i^L \rangle^L = \phi S^L (\langle \rho^L \rangle^L \langle e^L \rangle^L \langle v_i^L \rangle^L + \langle \rho^L \overset{\circ}{e}{}^L \overset{\circ}{v}_i{}^L \rangle^L)$$

$$= \langle \rho^L \rangle^L \langle e^L \rangle^L \langle v_i^L \rangle + \phi S^L \langle \rho^L \overset{\circ}{e}{}^L \overset{\circ}{v}_i{}^L \rangle^L \qquad \text{(A17)}$$

where the second term represents mechanical dispersion of energy. Following the current trend in the literature (c.f., Bear, 1972; Gray, 1975) we assume that dispersion is mathematically equivalent to a diffusion process, so that one can write

$$\langle \rho^L \overset{\circ}{e}{}^L \overset{\circ}{v}_i{}^L \rangle^L = - D_{ij}^L \frac{\partial \langle T^L \rangle^L}{\partial x_j} \qquad \text{(A18)}$$

where D_{ij}^L is known as the mechanical (or convective) dispersion tensor. The conductive flux, q_i^L, is expressed by Fourier's law using a scalar thermal conductivity,

$$q_i^L = - \kappa^L \frac{\partial T^L}{\partial x_i} \qquad \text{(A19)}$$

the average of which is given by (A9) as

$$\langle q_i{}^L \rangle = - \kappa^L \frac{\partial \langle T^L \rangle}{\partial x_i} - \frac{\kappa^L}{R} \int_{\Gamma^{LG}, \Gamma^{LS}} T^L n_i \, d\Gamma \qquad \text{(A20)}$$

In order to eliminate the surface integral from (A20) we assume that the orientation vector n_i is symmetrically distributed about a zero average value (this is true if the orientations of Γ^{LG} and Γ^{LS} are random). Then, since temperature is independent of interface orientation (i.e., random temperatures may exist at various points along Γ having a given orientation) T^L and n_i are uncorrelated and the surface integral in (A20) can be neglected. In a similar manner, it may appear reasonable to assume that $v_i{}^L n_i$ is symmetrically distributed about a zero average value along Γ^{LG} so that the first surface integral in (A16) vanishes. Similar considerations hold for the gas phase. If we further assume that ϕ, S^L, and S^G remain practically constant for any averaging volume whose centroid is

inside R, then (A16) can finally be reduced to

$$\frac{\partial}{\partial t}\left[\phi S^L \langle\rho^L\rangle^L \langle e^L\rangle^L + \phi S^G \langle\rho^G\rangle^G \langle e^G\rangle^G + (1-\phi)\,\rho^S \langle e^S\rangle^S\right]$$

$$= -\frac{\partial}{\partial x_i}\left(\langle\rho^L\rangle^L \langle e^L\rangle^L \langle v_i^L\rangle + \langle\rho^G\rangle^G \langle e^G\rangle^G \langle v_i^G\rangle\right)$$

$$+ \frac{\partial}{\partial x_i}\left[\phi S^L \kappa_{ij}^L \frac{\partial\langle T^L\rangle^L}{\partial x_j} + \phi S^G \kappa_{ij}^G \frac{\partial\langle T^G\rangle^G}{\partial x_j} + (1-\phi)\,\kappa^S \frac{\partial\langle T^S\rangle^S}{\partial x_i}\right]$$

$$- \langle p^L\rangle^L \frac{\partial\langle v_i^L\rangle}{\partial x_i} - \langle p^G\rangle^G \frac{\partial\langle v_i^G\rangle}{\partial x_i} \qquad \text{(A21)}$$

where $\kappa_{ij} = \kappa\delta_{ij} + D_{ij}$ is the combined conductive and mechanical dispersion tensor.

In the literature it is customary to assume that all phases are in thermal equilibrium and that capillary pressure differences between the fluid phases are negligible. In this case (A21) reduces to

$$\frac{\partial}{\partial t}\left[\phi S^L \langle\rho^L\rangle^L \langle e^L\rangle^L + \phi S^G \langle\rho^G\rangle^G \langle e^G\rangle^G + (1-\phi)\,\rho^S \langle e^S\rangle^S\right]$$

$$= -\frac{\partial}{\partial x_i}\left(\langle\rho^L\rangle^L \langle e^L\rangle^L \langle v_i^L\rangle + \langle\rho^G\rangle^G \langle e^G\rangle^G \langle v_i^G\rangle\right)$$

$$+ \frac{\partial}{\partial x_i}\left(\kappa_{ij}^{eff} \frac{\partial\langle T\rangle^*}{\partial x_j}\right) - \langle p\rangle^* \frac{\partial}{\partial x_i}\left(\langle v_i^L\rangle + \langle v_i^G\rangle\right) \qquad \text{(A22)}$$

where

$$\kappa_{ij}^{eff} = \phi S^L \kappa_{ij}^L + \phi S^G \kappa_{ij}^G + (1-\phi)\,\kappa^S \delta_{ij}$$

This shows that the assumption of thermal equilibrium implies viewing the solid, liquid, and gas as three anisotropic conductors arranged parallel to the direction of heat flow.

Recalling our assumption that thermodynamic relationships between average fluid properties are the same as between the equivalent point properties, we can define the average (macroscopic) enthalpy of the liquid as

$$\langle h^L\rangle^L = \langle e^L\rangle^L + \frac{\langle p^L\rangle^L}{\langle\rho^L\rangle^L} \qquad \text{(A24)}$$

Similar definitions will hold for the gas and the solid. If we now replace each $\langle e \rangle$ in (A22) by $\langle h \rangle - \langle p \rangle / \langle \rho \rangle$, we obtain a macroscopic energy equation in terms of enthalpy.

$$\frac{\partial}{\partial t} \left[\phi S^L \langle \rho^L \rangle^L \langle h^L \rangle^L + \phi S^G \langle \rho^G \rangle^G \langle h^G \rangle^G + (1 - \phi) \rho^S \langle h^S \rangle^S \right]$$

$$= - \frac{\partial}{\partial x_i} \left(\langle \rho^L \rangle^L \langle h^L \rangle^L \langle v_i^L \rangle + \langle \rho^G \rangle^G \langle h^G \rangle^G \langle v_i^G \rangle \right)$$

$$+ \frac{\partial}{\partial x_i} \left(\kappa_{ij}^{eff} \frac{\partial \langle T \rangle^*}{\partial x_j} \right) + \frac{\partial (\phi \langle p \rangle^*)}{\partial t} + (\langle v_i^L \rangle + \langle v_i^G \rangle) \frac{\partial \langle p \rangle^*}{\partial x_i} \qquad \text{(A25)}$$

Temperature Equation for a Single Phase

In the particular case where the pores are completely saturated by a single fluid phase (say liquid), one can use the equation of mass continuity to rewrite (A21) in the form

$$\phi \langle \rho^L \rangle^* \frac{\partial \langle e^L \rangle^*}{\partial t} + (1 - \phi) \rho^S \frac{\partial \langle e^S \rangle^S}{\partial t} = - \langle \rho^L \rangle^* \langle v_i^L \rangle \frac{\partial \langle e^L \rangle^*}{\partial x_i}$$

$$+ \frac{\partial}{\partial x_i} \left[\phi \kappa_{ij}^L \frac{\partial \langle T^L \rangle^*}{\partial x_j} + (1 - \phi) \kappa^S \frac{\partial \langle T^S \rangle^S}{\partial x_i} \right] - \langle p^L \rangle^* \frac{\partial \langle v_i \rangle^L}{\partial x_i} \qquad \text{(A26)}$$

Assuming that the thermodynamic relationships

$$\frac{\partial e}{\partial \bullet} = \left(\frac{\partial e}{\partial v} \right)_T \frac{\partial v}{\partial \bullet} + c_v \frac{\partial T}{\partial \bullet} \qquad \text{(A27)}$$

$$p = T \left(\frac{\partial p}{\partial T} \right)_v - \left(\frac{\partial e}{\partial v} \right)_T \qquad \text{(A28)}$$

hold for the average quantities appearing in (A26), this latter equation can be rewritten as

$$\left(\frac{\partial e^L}{\partial v}\right)_T \left[\phi<\rho^L>^* \frac{\partial(<\rho^L>^*)^{-1}}{\partial t} + <\rho^L>^* <v_i^L> \frac{\partial(<\rho^L>^*)^{-1}}{\partial x_i} - \frac{\partial <v_i^L>}{\partial x_i}\right]$$

$$+ \phi<\rho^L>^* c_v^L \frac{\partial <T^L>^*}{\partial t} + (1-\phi)\rho^S c_v^S \frac{\partial <T^S>^S}{\partial t}$$

$$= - <\rho^L>^* <v_i^L> c_v^L \frac{\partial <T^L>^*}{\partial x_i} + \frac{\partial}{\partial x_i}\left[\phi\kappa_{ij}^L \frac{\partial <T^L>^*}{\partial x_j} + (1-\phi)\kappa^S \frac{\partial <T^S>^S}{\partial x_i}\right]$$

$$- <T^L>^* \left(\frac{\partial p}{\partial T}\right)_v \frac{\partial <v_i^L>}{\partial x_i} \qquad \text{(A29)}$$

The first term in brackets can be reformulated as

$$- \frac{1}{<\rho^L>^*}\left[\phi \frac{\partial <\rho^L>^*}{\partial t} + \frac{\partial}{\partial x_i}(<\rho^L>^* <v_i^L>)\right]$$

which vanishes by virtue of mass continuity. Thus, the energy equation for the liquid phase can be expressed entirely in terms of temperature,

$$\phi<\rho^L>^* c_v^L \frac{\partial <T^L>^*}{\partial t} + (1-\phi)\rho^S c_v^S \frac{\partial <T^S>^S}{\partial t} = - <\rho^L>^* <v_i^L> c_v^L \frac{\partial <T^L>^*}{\partial x_i}$$

$$+ \frac{\partial}{\partial x_i}\left[\phi\kappa_{ij}^L \frac{\partial <T^L>^*}{\partial x_j} + (1-\phi)\kappa^S \frac{\partial <T^S>^S}{\partial x_i}\right] - <T^L>^* \left(\frac{\partial p}{\partial T}\right)_v \frac{\partial <v_i^L>}{\partial x_i}$$

(A30)

If the solid and the liquid are assumed to be in thermal equilibrium, (A30) reduces to

$$\left[\phi<\rho^L>^* c_v^L + (1-\phi)\rho^S c_v^S\right] \frac{\partial <T>^*}{\partial t} = - <\rho^L>^* <v_i^L> c_v^L \frac{\partial <T>^*}{\partial x_i}$$

$$+ \frac{\partial}{\partial x_i}\left(\kappa_{ij}^{eff} \frac{\partial <T>^*}{\partial x_j}\right) - <T>^* \left(\frac{\partial p}{\partial T}\right)_v \frac{\partial <v_i^L>}{\partial x_i} \qquad \text{(A31)}$$

where $\kappa_{ij}^{eff} = \phi\kappa_{ij}^L + (1-\phi)\kappa^S \delta_{ij}$.

Equations A30 and A31 are also applicable when the pores are completely saturated by the gas phase, provided that the superscript L is replaced by G.

REFERENCES

Anand, J., W. H. Somerton and E. Gomaa, 1973, Predicting thermal conductivities of formations from other known properties, Soc. Petrol. Engr. Jour., v. 13, no. 5, pp. 267-273.

Bear, J., 1972, Dynamics of Fluids in Porous Media, Am. Elsevier, New York.

Beck, J. L., 1972, Convection in a box of porous material saturated with fluid, Phys. of Fluids, v. 15, no. 8, pp. 1377-1383.

Billhartz, H. L., Jr., 1971, Fluid Production from Geothermal Steam Reservoirs, M. S. thesis, Stanford Univ., Calif.

Bodvarsson, G., 1961, Physical characteristics of natural heat resources in Iceland, paper G.6, U. N. Conf. on New Sources of Energy, Rome, August 21-31.

Brace, W. F., J. B. Walsh and W. T. Francos, 1968, Permeability of granite under high pressure, Jour. Geophys. Research, v. 73, no. 6, pp. 2225-2236.

Brigham, W. E. and W. B. Morrow, 1974, P/Z behavior for geothermal steam reservoirs, paper SPE 4899, 44th Annual Calif. Regional Meeting SPE-AIME, San Francisco, April 4-5.

Brownell, D. H., Jr., S. K. Garg and J. W. Pritchett, 1975, Computer simulation of geothermal reservoirs, paper SPE 5381, 45th Annual Calif. Regional Meeting SPE-AIME, Ventura, Calif. April 2-4.

Cady, G. V., 1969, Model Studies of Geothermal Fluid Production, Ph.D. dissertation, Stanford Univ., Calif.

Calhoun, J. C., M. Lewis, Jr. and R. C. Newman, 1949, Experiments on the capillary properties of porous solids, Trans. AIME, v. 186, pp. 189-196.

Caltagirone, J. P., M. Cloupeau and M. Combarnous, 1971, Convection naturelle fluctuante dans une couche poreuse horizontale, Comptes Rendus, Acad. Sci., Paris, B273, pp. 833-836.

Casse, F. J., 1974, The Effect of Temperature and Confining Pressure on Fluid Flow Properties of Consolidated Rocks, Stanford Geothermal Program, Rep. SGP-TR3, Stanford Univ., Calif.

Cheng, P. and K. H. Lau, 1974, Steady state free convection in an unconfined geothermal reservoir, Jour. Geophys. Res., v. 79, no. 29, pp. 4425-4431.

Coats, K. H., W. D. George, C. Chu and B. E. Marcum, 1974, Three-dimensional simulation of steamflooding, Soc. Petrol. Engr. Jour., v. 15, no. 6, pp. 573-592.

Combarnous, M. A. and S. A. Bories, 1973, Thermal Convection in Saturated Porous Media, Report prepared for Advances in Hydroscience, Institut Francais du Petrole and Institute de Mecanique des Fluides de Toulouse.

Combarnous, M. and S. Bories, 1974, Modelisation de la convection naturelle au sein d'une couche poreuse horizontale a l'aide d'un coefficient de transfert solide-fluide, Int. Jour. Heat Mass Transfer, v. 17, pp. 505-515.

Craig, H., 1966, Superheated steam and mineral-water interactions in geothermal areas, Trans. Am. Geophys. Union, v. 47, pp. 204-205 (abstract).

Currie, I. G., 1974, Fundamental Mechanics of Fluids, McGraw-Hill, New York.

Davidson, L. B., 1969, The effect of temperature on the permeability ratio of different fluid pairs in two-phase systems, Jour. Petrol. Tech., Aug. 1969, pp. 1037-1046.

Donaldson, I. G., 1962, Temperature gradients in the upper layers of the earth's crust due to convective water flows, Jour. Geophys. Res., v. 67, no. 9, pp. 3449-3459.

Donaldson, I. G., 1968a, The flow of steam water mixtures through permeable beds: A simple simulation of a natural undisturbed hydrothermal region, New Zealand Jour. Sci., v. 11, pp. 3-23.

Donaldson, I. G., 1968b, A possible model for hydrothermal systems and methods of studying such a model, paper 2580, Third Australian Conf. on Hydraulics and Fluid Mechanics, Nov. 25-29.

Donaldson, I. G., 1970, The simulation of geothermal systems with a simple convective model, Geothermics, Special issue 2, v. 2, part 1, pp. 649-654.

Edmonson, J. A., 1965, Effect of temperature on waterflooding, Jour. Canadian Petrol. Tech., v. 4, no. 4, pp. 236-242.

Einarsson, T., 1942, Ueber das Wesen der heissen Quellen Islands, Rit. Vísind. Ísl., v. 26, 91 p.

Elder, J. W., 1965, Physical processes in geothermal areas in Terrestrial Heat Flow, W. H. K. Lee, ed., Am. Geophys. Union Mon., ser. 8, pp. 211-239.

Elder, J. W., 1966, Heat and mass transfer in the earth: Hydrothermal systems, New Zealand D.S.I.R. Bull. 169, 115 p.

Elder, J. W., 1967, Transient convection in a porous medium, Jour. Fluid Mech., v. 27, part 3, pp. 609-623.

Facca, G. and F. Tonani, 1964, Theory and technology of a geothermal field, Bull. Volcanol., v. 27, part 1, pp. 143-189,

Faust, C. F. and J. W. Mercer, 1975, Mathematical modeling of geothermal systems, paper to be presented at Second United Nations Symposium on the Development and Use of Geothermal Resources, San Francisco, May 20-29.

Fernandez, R. T., 1972, Natural Convection from Cylinders Buried in Porous Media, Ph.D. dissertation, Univ. of Calif., Berkeley.

Goguel, J., 1953, Le regime thermique de l'eau souterraine, Annales des Mines, v. 10, pp. 3-32.

Gray, W. G., 1975, A derivation of the equations for multi-phase transport, paper submitted to Chem. Engr. Sci.

Greenberg, D. B., R. S. Cresap and T. A. Malone, 1968, Intrinsic permeability of hydrological porous mediums: Variation with temperature, Water Resour. Res., v. 4, no. 4, pp. 791-800.

Gringarten, A. C. and J. P. Sauty, 1975, A theoretical study of heat extraction from aquifers with uniform regional flow, paper submitted to Jour. Geophys. Res.

Gupta, V. P. and D. D. Joseph, 1973, Bounds for heat transport in a porous layer, Jour. Fluid Mech., v. 57, part 3, pp. 491-514.

Haas, J. L., Jr., 1970, An equation for the density of vapor-saturated NaCl-H_2O solutions from 75° to 325°C, Am. Jour. Sci., v. 269, pp. 489-493.

Haas, J. L., Jr., 1971, The effect of salinity on the maximum thermal gradient of a hydrothermal system at hydrostatic pressure, Econ. Geol., v. 66, pp. 940-946.

Helgeson, H. C., 1968, Geologic and thermodynamic characteristics of the Salton Sea geothermal system, Am. Jour. Sci., v. 266, pp. 129-166.

Holst, P. H., 1970, A Theoretical and Experimental Investigation of Natural Convection in Porous Media, Ph.D. dissertation, Univ. of Calgary, Alberta, Canada.

Holst, P. H. and K. Aziz, 1972a, A theoretical and experimental study of natural convection in a confined porous medium, Canadian Jour. Chem. Engr., v. 50, pp. 232-241.

Holst, P. H. and K. Aziz, 1972b, Transient three-dimensional natural convection in confined porous media, Jour. Heat and Mass Transfer, v. 15, pp. 73-90.

Horne, R. N. and M. J. O'Sullivan, 1974, Oscillatory convection in a porous medium heated from below, Jour. Fluid Mech., v. 66, part 2, pp. 339-352.

Horton, C. W. and F. T. Rogers, Jr., 1945, Convection currents in a porous medium, Jour. Appl. Phys., v. 16, no. 6, pp. 367-370.

James, R., 1968, Wairakei and Lardarello geothermal power systems compared, New Zealand Jour. Sci. and Tech., v. 11, pp. 706-719.

Jeffreys, H., 1930, The instability of a compressible fluid heated below, Proc. Cambridge Phil. Soc., v. 26, pp. 170-172.

Kaneko, T., M. F. Mohtadi and K. Aziz, 1974, An experimental study of natural convection in inclined porous media, Int. Jour. Heat Mass Transfer, v. 17, pp. 485-496.

Kapplemeyer, O. and R. Haenel, 1974, Geothermics with Special Reference to Application, Geopublication Associates, Berlin, tables 6.3-6.6, pp. 208-218.

Karra, P. S., 1968, A numerical Study of Natural Convection in Porous Media, M. S. thesis, Univ. of Calgary, Alberta, Canada.

Knutson, C. F. and B. F. Bohor, 1963, Reservoir rock behavior under moderate confining pressure in Symposium on Rock Mechanics, Univ. Minnesota, MacMillan, New York, pp. 627-659.

Lapwood, E. R., 1948, Convection of a fluid in a porous medium, Proc. Cambridge Phil. Soc., v. 44, pp. 508-521.

Lasseter, T. J. and P. A. Witherspoon, 1974, Underground Storage of Liquified Natural Gas in Cavities Created by Nuclear Explosives, Geotechnical Engineering Pub. No. 74-1, Univ. Calif., Berkeley.

Lasseter, T. J., P. A. Witherspoon and M. J. Lippmann, 1975, Multiphase multi-dimensional simulation of geothermal reservoirs, paper submitted to Second United Nations Symposium on the Development and Use of Geothermal Resources, San Francisco, May 20-29.

Lee, P. C. Y., W. G. Gray and G. F. Pinder, 1975, Thermoenergy transport in porous media, paper in preparation.

Likke, S. and L. A. Bromley, 1973, Heat capacities of aqueous NaCl, KCl, $MgCl_2$ $MgSO_4$, and Na_2SO_4 solutions between 80° and 200°C, Jour. Chem. Engr. Data, v. 18, no. 2, pp. 189-195.

Lo, H. Y. and N. Mungan, 1973, Effect of temperature on water-oil relative permeabilities in oil-wet and water-wet systems, paper SPE 4505, 48th Annual Meeting SPE-AIME, Las Vegas, Nev., Sept. 30-Oct. 3.

Marinelli, G., 1969, Some geological data on the geothermal areas of Tuscany, Bull. Volcanol., v. 33, no. 1, pp. 319-334.

Martin, J. C., 1975, Analysis of internal steam drive in geothermal reservoirs, paper SPE 5382, 45th Annual Calif. Regional Meeting SPE-AIME, Ventura, Calif., April 2-4.

Masouka, T., 1972, Heat transfer by free convection in a porous layer heated from below, Heat Transfer-Japan Res., v. 1, no. 1, pp. 39-45.

Matthews, C. S. and D. G. Russell, 1967, Pressure Buildup and Flow Tests in Wells, Soc. Petr. Engr. AIME Mon., v. 1.

McNabb, A., 1965, On convection in a porous medium, Proc. Australasian Conf. on Hydraulics and Fluid Mechanics, v. 2, pp. C161-C171.

Mercer, J. W., Jr., 1973, Finite Element Approach to the Modeling of Hydrothermal Systems, Ph.D. dissertation, Univ. of Illinois, Urbana-Champaign.

Mercer, J. W., Jr., C. F. Faust and G. F. Pinder, 1974, Geothermal reservoir simulation, Proc. NSF Conference on Research for the Development of Geothermal Energy Resources, Pasadena, Calif., Sept. 23-25, pp. 256-267.

Mercer, J. W. and G. F. Pinder, 1974, Finite element analysis of hydrothermal systems, in Finite Elements in Fluid Flow, J. T. Oden, et al., eds., Univ. Alabama Huntsville Press, pp. 401-414.

Mercer, J. W., G. F. Pinder and I. G. Donaldson, 1975, A Galerkin-finite element analysis of the hydrothermal system at Wairakei, New Zealand, Jour. Geophys. Res., in press.

Narasimhan, T. N. and P. A. Witherspoon, 1975, An integrated finite difference method for analyzing fluid flow in porous media, paper submitted to Water Resour. Res.

Nevens, T. O. and M. J. Pool, 1964, Determination of Thermodynamic Properties of Brines, Denver Research Inst., Contract Research Report 2151.

Nield, D. A., 1968, Onset of thermohaline convection in a porous medium, Water Resour. Res., v. 4, no. 3, pp. 553-560.

Nield, D. A., 1974, Comments on 'Effect of solute dispersion on thermal convection in a porous medium layer' by H. Rubin, Water Resour. Res., v. 10, no. 4, p. 889.

Palm, E., J. E. Weber and O. Kvernvold, 1972, On steady convection in a porous medium, Jour. Fluid Mech., v. 54, part 1, pp. 153-161.

Platzman, G. W., 1965, The spectral dynamics of laminar convection, Jour. Fluid Mech., v. 23, part 3, pp. 481-510.

Poston, S. W., S. C. Ysrael, A. K. M. S. Hossain, E. F. Montgomery, III and H. J. Ramey, Jr., 1970, The effect of temperature on irreducible water saturation and relative permeability of unconsolidated sands, Soc. Petrol. Eng. Jour., v. 10, no. 2, pp. 171-180.

Ramey, H. J., Jr., W. E. Brigham, H. K. Chen, P. G. Atkinson and N. Arihara, 1974, Thermodynamic and hydrodynamic properties of hydrothermal systems, in The Utilization of Volcano Energy, J. L. Colp and A. S. Furumoto, eds., Proc. of Converence, Hilo, Hawaii, Feb. 4-8.

Ramey, H. J., Jr., P. Kruger and R. Raghavan, 1973, Explosive stimulation of hydrothermal reservoirs in Geothermal Energy, P. Kruger and C. Otte, eds., Stanford Univ. Press, pp. 231-249.

Rayleigh, Lord, 1916, On convection currents in a horizontal layer of fluid when the higher temperature is on the underside, Phil. Mag., Ser. 6, v. 32, pp. 529-246.

Rubin, H., 1973, Effect of solute dispersion on thermal convection in a porous medium layer, Water Resour. Res., v. 9, no. 4, pp. 968-974.

Rubin, H., 1975a, Effect of solute dispersion on thermal convection in a porous medium layer, 2, Water Resour. Res., v. 11, no. 1, pp. 154-158.

Rubin, H., 1975b, On the analysis of cellular convection in porous media, Unpublished manuscript.

Rubin, H., 1975c, Effect of hydrodynamic dispersion on thermohaline convection in a porous medium, Unpublished manuscript.

Sanyal, S. K., S. S. Marsden and H. J. Ramey, Jr., 1972, The effect of temperature on electrical resistivity of porous media, Soc. Prof. Well Logging Assoc., 13th Annual Logging Symposium, May 1972.

Sestini, G., 1970, Superheating of geothermal steam, Geothermics, Special issue 2, v. 2, pt. 1, pp. 622-648.

Slattery, J. C., 1972, Momentum, Energy and Mass Transfer in Continua, McGraw-Hill, New York.

Somerton, W. H., J. A. Keese and S. L. Chu, 1974, Thermal behavior of unconsolidated oil sands, Soc. Petrol. Engr. Jour., v. 14, no. 5, pp. 513-521.

Sorey, M. L., 1975, Numerical Modeling of Liquid Geothermal Systems, Ph.D. dissertation, Univ. of Calif., Berkeley (in preparation).

Spillette, A. G. and R. L. Nielsen, 1968, Two-dimensional method for predicting hot waterflood recovery behavior, Jour. Petrol. Tech., v. 20, no. 6, pp. 627-638.

Straus, J. M., 1974, Large amplitude convection in porous media, Jour. Fluid Mech., v. 64, part 1, pp. 51-63.

Sun, Z. S., C. Tien and Y. C. Yen, 1972, Onset of convection in a porous medium containing liquid with a density maximum, paper NC2-11, Fourth Intern. Heat Transfer Conf., Paris-Versailles, v. 4.

Toronyi, R. M., 1974, Two-Phase, Two-Dimensional Simulation of a Geothermal Reservoir and the Wellbore System, Ph.D. dissertation, Pennsylvania State Univ., University Park.

Vairogs, J., C. L. Hearn, D. W. Dareing and V. W. Rhoades, 1971, Effect of rock stress on gas production from low-permeability reservoirs, Jour. Petrol. Tech., Sept. 1971, pp. 1161-1167.

Wankat, P. C. and W. R. Schowalter, 1970, Stability of combined heat and mass transfer in a porous medium, Phys. of Fluids, v. 13, no. 9, pp. 2418-2420.

Weber, J. E., 1975a, Thermal convection in a tilted porous layer, Int. Jour. Heat Mass Transfer, v. 18, pp. 474-475.

Weber, J. E., 1975b, The boundary-layer regime for convection in a vertical porous layer, Int. Jour. Heat Mass Transfer, v. 18, pp. 659-573.

Weinbrandt, R. M., H. J. Ramey, Jr. and F. J. Casse, 1972, The effect of temperature on relative and absolute permeability of sandstones, 47th Annual Meeting SPE-AIME, San Antonio, Texas, Oct. 1972.

Weinstein, H. G., J. A. Wheeler and E. G. Woods, 1974, Numerical model for steam stimulation, paper SPE 4759, SPE-AIME Improved Oil Recovery Symposium, Tulsa, Oklahoma, April 22-24.

Westbrook, D. R., 1969, Stability of convective flow in a porous medium, Phys. of Fluids, v. 12, no. 8, pp. 1547-1551.

Whitaker, S., 1968, Introduction to Fluid Mechanics, Prentice-Hall, Englewood Cliffs, N. J.

Whitaker, S., 1969, Advances in theory of fluid motion in porous media, Ind. Engr. Chem., v. 61, no. 12, pp. 14-28.

White, D. E., 1957, Thermal waters of volcanic origin, Bull. Geol. Soc. Am., v. 68, pp. 1637-1658.

White, D. E., 1961, Preliminary evaluation of geothermal areas, paper G.2, U. N. Conf. on New Sources of Energy, Rome, August 21-31.

White, D. E., 1973, Characteristics of geothermal resources, in Geothermal Energy, P. Kruger and C. Otte, eds., Stanford Univ. Press, pp. 69-94.

White, D. E., L. J. P. Muffler and A. H. Truesdell, 1971, Vapor-dominated hydrothermal systems compared with hot-water systems, Econ. Geol., v. 66, pp. 75-97.

Whiting, R. L. and H. J. Ramey, Jr., 1969, Application of material and energy balances to geothermal steam production, Jour. Petrol. Tech., v. 21, no. 7, pp. 893-900.

Wooding, R. A., 1963, Convection in a saturated porous medium at large Rayleigh number or Péclet number, Jour. Fluid Mech., v. 15, part 4, pp. 527-544.

Yen, Y. C., 1974, Effects of density inversion on free convective heat transfer in porous layer heated from below, Int. Jour. Heat Mass Transfer, v. 17, pp. 1349-1356.

Zoback, M. D. and J. D. Byerlee, 1975, Permeability and effective stress, AAPG Bull., v. 59, no. 1, pp. 154-158.

TECHNICAL INFORMATION DIVISION
LAWRENCE BERKELEY LABORATORY
UNIVERSITY OF CALIFORNIA
BERKELEY, CALIFORNIA 94720